Joint European MSc Degree
European MSc in Marine Environment and

MER QUALITY AWARD MICINN 2008-2012
MO2006-00744

Ref

MASTER THESIS PROJECT

A mechanistic study of the low trophic level ecosystem structure in the coastal zone

Presented by: **Giulia Mussap**

Supervisor: Prof. **Nadia Pinardi**

Co-supervisor: Dott. **Marco Zavatarelli**

SiNCEM Laboratory, Scienze Ambientali, University of Bologna

Plentzia (UPV/EHU), September 2012

Universidad del País Vasco Euskal Herriko Unibertsitatea
UNIVERSITY OF Southampton
UNIVERSITÉ BORDEAUX 1
azti tecnalia

Per il mio cuore basta il tuo petto,
per la tua libertà bastano le mie ali.
Dalla tua bocca arriverà fino al cielo
ciò che stava sopito sulla mia anima.

E' in te l'illusione di un giorno.
Giungi come rugiada sulle corolle.
Scavi l'orizzonte con la tua assenza,
Eternamente in fuga come l'onda.

Ho detto che cantavi nel vento
come i pini e come gli alberi maestri delle navi.
Come quelli sei alta e taciturna.
E di colpo ti rattristi, come un viaggio.

Accogliente come una vecchia strada.
Ti popolano echi e voci nostalgiche.
Io mi sono svegliato e a volte migrano e fuggono
gli uccelli che dormivano nella tua anima.

A nonna Elda e nonno Giorgio...

Abstract

The coastal area is of particular interest due to its high productivity, the affluence of freshwater and nutrients from land, and the global carbon flux. In the pelagic marine environment, two contrasting pathways of the flux of biogenic carbon from autotrophic to heterotrophic organisms have been defined: the herbivorous and the microbial food webs (Legendre and Rassoulzadegan, 1995). Physical characteristics of the water column define the food web of a particular area: mixing stimulates the herbivorous food web while stratification favours the microbial food web. We aim at understanding the low trophic level ecosystem structure in a typical estuarine Gulf such as the Gulf of Trieste (Italy). The coupling of the numerical models Princeton Ocean Model (1D) and the Biogeochemical Flux Model (BFM) enables to study how the trophic chain works in a typical estuary such as the Gulf of Trieste (Italy). Statistical analysis was performed on data following the year 2000 in order to force the initial physical data in the model and compare other variables with model results. Two experiments were then performed to investigate the microbial role in the carbon cycling that determines differences between the microbial pathway and the herbivore pathway, and to investigate the competition between plankton and bacteria on nutrients cycling. The experiments tested the model sensitivity with different closure remineralization rates when bacteria were removed from the system and when all the microbial system was isolated. Results demonstrated the high model sensitivity for small changes and therefore the reliability. We show how bacteria play a major role in the definition of the local food web by competing with phytoplankton. Also, we find that when bacteria and the whole microbial system are remove the system shifts from P-limited to N-limited and from "bottom-up" to "top-down" control.

Contents

Chapter 1

Introduction

1.1 The coastal zone

The coastal ocean accounts for 7% of the ocean surface areas, <0.5% of the ocean's volume and between 10 and 20% of the global ocean production. It plays a major role in the global organic matter burial (80%), in the global sedimentary mineralization (90%) and in the global sink of suspended river load (75-90%). Furthermore, it contributes to >50% of present day global carbonate deposition.

The coastal areas are a largely studied part of the global ocean, due to their susceptibility to changes in water quality, organic productivity and biodiversity (Mackenzie et al., 2004). It is the junction point in the biosphere where the land, ocean and atmospheric components of the planetary biogeochemical system meet and interact (Ducklow and McCallister, 2004). The connection between the land and sea is provided by river runoff and groundwater discharge. The land-derived inputs to the sea are constrained by the runoff and by the amount of material transported; the former being mostly dependent on climate dynamics, while the latter strongly influenced by anthropogenic factors. In such transport process, anthropogenic (pollutant) flows superimpose to natural flows. The nutrient load to the coastal ocean has increased dramatically over the past 300 years and the ratio of Si:N:P has changed as well (Platt et al., 2004). Changes in nutrient loading and nutrient supply ratio may lead to shifts in phytoplankton community composition as well as bottom anoxia and hypoxia, and light limitation. The net transfer of organic matter across the interfaces dictates the metabolic balance of the coastal ocean (Ducklow and McCallister, 2004). In general, interfaces between earth system components (i.e. the land, atmosphere and ocean) are important in the control of biogeochemical cycles.

The driving force of the organic carbon cycle in the global ocean is the production of organic matter (OM) by marine primary producers (Mackenzie et al., 2004).

The nutrient rich river runoff in the shallow coastal oceans makes the coastal zone a very productive region relative to that of average oceanic surface waters. The magnitude of primary production, respiration, decay and the physical transport processes control the carbon flux between reservoirs of the global marine organic carbon cycle. Biogeochemical processing in estuaries is the primary control regulating the relocation of terrigenous OM from land to the coastal ocean. OM loadings from the land also influence the carbon balance in the coastal ocean and thus affects its source/sink characteristics (Ducklow and McCallister, 2004).

Primary production in the coastal ocean, as in the open sea, is dominated by unicellular phytoplankton, but the composition and physiology of the flora and the relative importance of nutrients, light and grazing as limiting factors on phytoplankton growth differ in important ways from the open sea (Ducklow and McCallister, 2004). N, P and micronutrients inputs via river runoff are accompanied by dissolved inorganic carbon (DIC) and support primary production. In fact, phytoplankton growth requires the macronutrients N and P for biosynthesis of proteins, nucleic acids, phospholipids and micronutrients which serve as co-factors in enzymes. In addition to these nutrients, diatoms require Si for their cell walls (frustles) (Platt et al., 2004). Coastal ocean systems have higher stocks and production of both large and small phytoplankton, compared to the open sea, resulting in higher biomass and a greater proportion of large forms. These consequently sink more rapidly exporting surface production at depth more efficiently.

It is generally accepted that phytoplankton dynamics are, ultimately, under control of physical forcing (Platt et al., 2004). These control and influence the initiation of the blooms which are events coonected to fisheries and harmful algae blooms.

1.2 Physical characteristics

Within coastal ecosystems, interactions among intertidal, benthic and pelagic communities enhance nutrient cycles and primary productivity. These interactions are, directly or indirectly, enabled or constrained by physical processes (currents, waves, turbulent mixing, pycnoclines and fronts) that structure pelagic ecosystems and resonate with biological processes over a broad spectrum of time-space scales (hours - decades, meters to thousands of kilometers) (PICO, 2012).

In coastal and shelf seas the lateral boundaries effects play a crucial role in the ocean dynamics. Stratifying influences compete with mixing influences to crontrol the vertical structure of the water column on time scales of hours to seasons. In contrast to the open ocean, the coastal zone is strongly influenced by bathymetry and geometry,

and can be dominated by tides. Local freshwater inputs from major rivers influence mixing and heat exchange with the atmosphere, as does the wind. Generally, most of the coastal circulation is dominated by tidal and wind-driven currents. Figure 1.1 represents a schematic of the processes taking place in a typical coastal area which is divided from the open ocean by the shelf break.

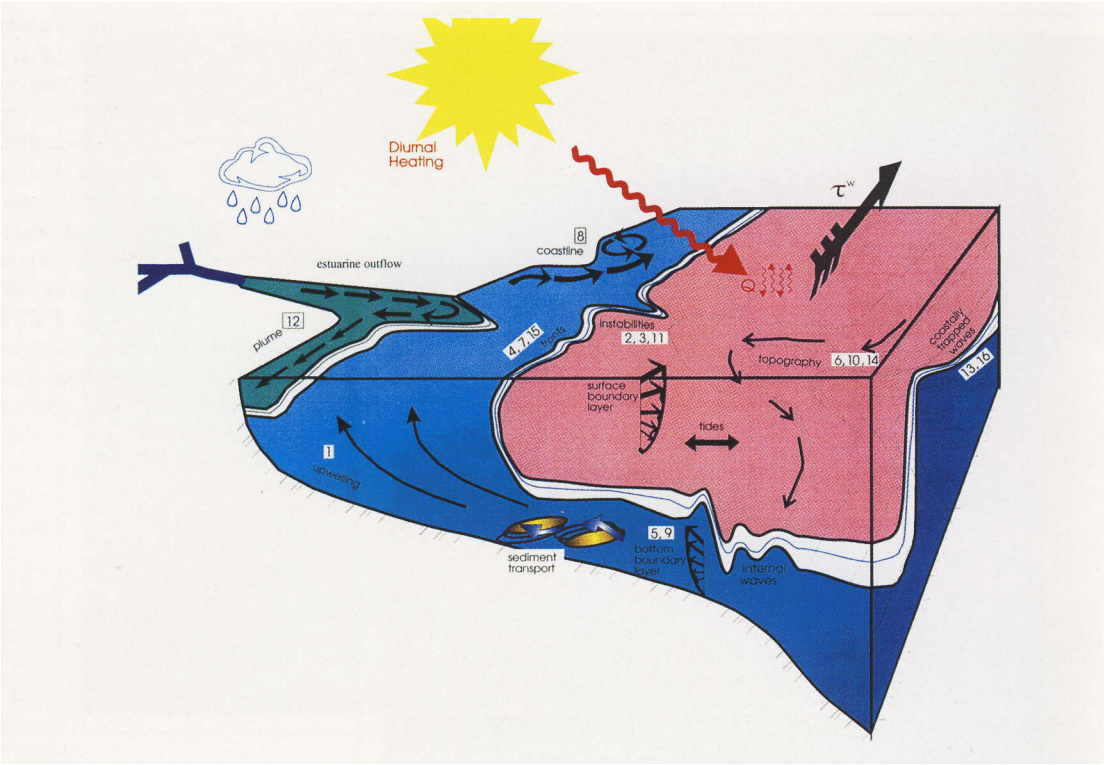

Figure 1.1: A schematic of the physical processes taking place in a typical coastal area (Dickey et al., 1998)

The stratification of the ocean is broken through mixing. As figure 1.1 shows, many processes in the coastal area are linked together and contribute to the mixing of the water column, some of them being the wind driven coastal upwelling, river inputs, groundwater input, currents (tidal), waves and friction. Tidal mixing is one of the leading processes contributing significantly to the generation of turbulence: it is persistent and constant, and involve the movement of large quantities of water between the open sea and the coast. Wind driven currents and waves also generate mixing at different levels, depending on wind intensity and direction. Strong winds can influence the surface circulation in coastal areas and sometimes even reverse it. The currents resulting from these different forcings are subject to the Ekman transport, resulting in situations of upwelling or downwelling.

Although upwelling is not a process present in all coastal zones, in those where it is, it is often the dominant coastal process. Maximum upwelling occurs when the wind

is parallel to the shore and it produces the surfacing of the pycnocline. Upwelling is significant not only for the fact that it contributes to mixing and brings deep, cold water to the surface, but also because this deep water is rich in nutrients. The process is therefore also very important for primary production. Upwelling also causes currents on the seafloor towards the coast and bottom friction causes turbulence resulting in a bottom boundary layer where properties of the water column are mixed.

Stratification in the coastal zone on the other hand is favoured by river discharge and surface heating. Freshwater delivered by rivers causes a salinity decrease in the coastal area and this results in a gradient of increasing salinity from the coast towards the open ocean. Since riverine freshwater is less dense than the saline coastal water, it floats on the surface increasing the stability of the water column and favouring stratification. Moreover, river input is normally stronger during the cold months, when precipitation is heavier. Contrastingly, heating plays a fundamental role during the summer hot months creating a strong thermocline. Moreover, heating causes evaporation and this may result in shelf water becoming saltier and therefore denser than the adjacent oceanic water. This is defined as a dense water cascade and may also result from the cooling of the shelf water. It is an important process for the transport of water off the shelf.

Another important process in shelf areas are shelf waves like seiches and Kelvin waves. These influence the coastal circulation and respond to atmospheric forcing. In fact they can form as a consequence of a storm and when the wind influence stops, they can continue to slosh back and forth for some time after the storm has stopped. This behavior consequently influences the circulation in the area and the mixing in the water column.

1.3 The trophic structure

Coastal and ocean trophic systems are of particular interest due to their role as atmospheric CO_2 sinks via primary production. The term "biological pump" refers to the carbon sequestration process where inorganic carbon in the atmosphere is fixed during photosynthesis of primary producers and transformed into OM. This is then subject to foodweb processes and is transported via mixing and transport to the interior of the ocean. However, the atmospheric CO_2 absorbed by coastal ocean processes will only enter long-term storage if it is transported laterally offshore to the ocean interior (Ducklow and McCallister, 2004). Walsh (1991) calculated that the coastal ocean contributed to 50% of the total oceanic particle flux at a depth of 2650m as a consequency of this process.

In the pelagic marine environment, biological oceanographers generally distinguish between two contrasting pathways of the flux of biogenic carbon from autotrophic to heterotrophic organisms: the herbivorous and the microbial food webs (Legendre and Rassoulzadegan, 1995). The herbivorous food web develops in conditions where the vertically mixed water colum is stabilized (such as upwelling areas) and high amplitude diatom blooms develop. Large diatoms consequently stimulate the herbivorous zooplankton community and this then generally favours a food web leading to large animals and fish. Contrastingly, the production of small phytoplankton (pico- and nanoplankton) leads to the microbial food web constitued by phototrophic cells, heterotrophic bacteria and protozoa. Figure 1.2 summarises the conditions which lead to the different paths resulting in either the herbivorous food web or the microbial web. Starting with the water column hydrodynamics, which controls nutrient availability and therefore the type of phytoplankton production (new or regenrated) and organisms (large or small cells). This then leads to a specific food web (herbivorous or microbial) and finally to the type of pelagic ecosystem (coastal or oceanic).

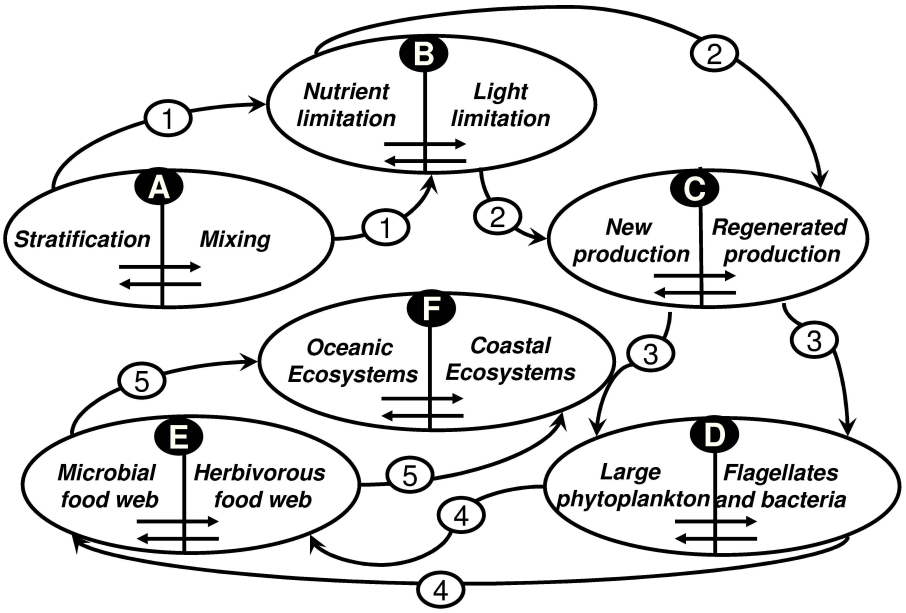

Figure 1.2: Schematic representation of the conditions leading to either a coastal or oceanic pelagic ecosystem.Se sequence comprises of the water column vertical structure (A), the factors limiting growth (B), the type of primary production (C), the type of organisms (D), the resulting food web (E) and the type of ecosystem (F). (After Pinardi et al. (2005))

Phytoplankton and heterotrophic bacteria, as primary producers and decomposers, form the basis of aquatic systems largely controlling pelagic energy flow and nutrient cycling (Danger et al., 2007a). Different environmental conditions (light, carbon and nutrient inputs) influence the relationship between them which may shift from net

mutualism or commensalism to net competition. In fact, in the case where bacteria feed on dissolved and particulate organic carbon (DOC and POC) poor of essential nutrients such a nitrogen or phosphorus, in order to equilibrate their chemical composition they must take up free mineral nutrients from the environment (Kirchman, 1994). Jansson (1988) argues that bacteria have higher affinity for phosphate, but they are energy-limited rather than phosphate-limited and depend on algal organic exudates for their energy supply.

Cushing (1989) argues that the microbial web predominates in stratified waters because the exudates from small phytoplankton are not dispersed and can therefore be used by heterotrophic bacteria. Azam and Ammerman (1984) hypothesized that phytoplankton exudation has evolved a mechanism establishing small-scale feedback interactions (mutualism) with bacteria, i.e. phytoplankton provide reduced carbon for bacteria, while these produce remineralized nutrients for phytoplankton. In such a case, phytoplankton production would be regulated by feedback interactions, which optimize the use of dissolved inorganic nutrients at low concentrations. Jumars et al. (1989) argued that phytoplankton exudations not the only source of DOM for bacterial production and that faecal pellets lose DOC and dissolved organic nitrogen (DON) very rapidly following egestion. This consequently causes the labile solutes to remain in the upper mixed layer. The most steady sources of DOM for bacteria are thus probably exudation by phytoplankton and diffusion from sinking faecal pellets (Legendre and Rassoulzadegan, 1995). It has been hypothesized (Caron et al., 1988) that when the available DON runs low, bacteria will cease from releasing ammonium and become competitors of phytoplankton. In such a case, the microbial loop would dominate.

Microbes also play a fundamental role in the recycling of OM and nutrients as the energy is transferred above the thermocline stimulating the growth of primary producers.

The microbial loop concept refers to the production of DOM in aquatic food webs during the flux of particulate matter towards larger organisms, and the reincorporation of this DOM by heterotrophic bacteria and archaea (Pernthaler, 2005). These mainly live in carbon-based matter either individually, in filaments or a large population forming hotspots known as marine snow. Studies to understand the microbial carbon pump-mediated carbon sequestration must contend with great molecular and microbial diversity and system complexity - as well as minuscle, nanometer to micrometer, ecosystem scales relevant to the realms of microbes and molecules (Jiao and Azam, 2011). The development of the thechnique of epifluorescence microscopy marked a turning point for the comprehension of the microbial loop. In fact, previous methods had missed >99% of microorganisms and had grossly underestimated their metabolism

(Azam, 1998).

Bacteria are a critical part of the marine food web and it is now well established that the flux of organic matter into bacteria is a major pathway. About one-half of oceanic primary production on average is channeled via bacteria into the microbial loop (Azam et al., 1983). A general trend of increasing bacterial number and biomass with increasing primary productivity and seasonal patterns were observed by Azam et al. (1983) in response to DOM released by phytoplankton. Major fluxes of organic matter move via DOM into bacteria and the microbial loop , which then returns the energy initially released as DOM by phytoplankton (figure 1.3). Therefore, the DOM-bacteria flux has fundamental implications for the overall carbon flux patterns (Azam, 2000).

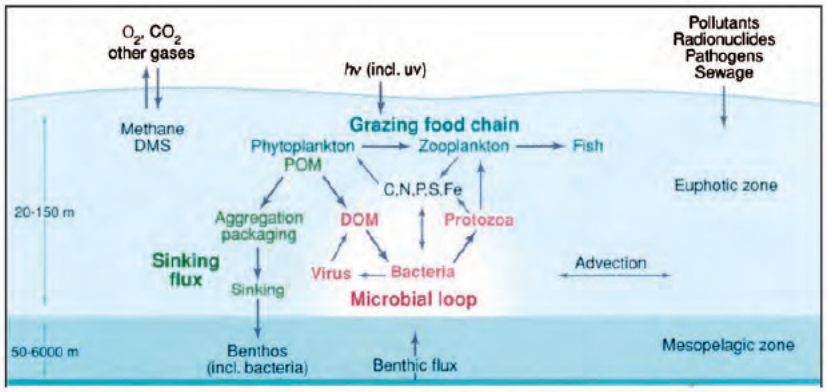

Figure 1.3: The modern view of the pelagic foodweb with the microbial loop playing a major role for the organic matter flux (After Azam (1998))

Bacterioplankton represent the largest living surface in the world's oceans and might exceed phytoplankton biomass even in the euphotic zone of oligotrophic regions (Cho and Azam, 1990). There is, however, still considerable uncertainty about the fraction of the bacterial community metabolically active at a given time (Stoderegger and Herndl, 1998). A few studies reported that microorganisms also produce DOM that is resistant to decomposition (Stoderegger and Herndl, 1998).

Bidle and Azam (1999) found that bacteria-mediated silicon regeneration is of quantitative significance for oceanic diatom biogeochemistry. They observed that silicon regeneration apperared to be controlled by colonization intensity rather than bulk-phase bacterial abundance. Therefore, the microbial loop may also exert critical controls on diatom production and its biogeochemical fate.

The main source of microbial mortality in the water column are currently considered to be viral-mediated lysis and grazing by phagotrophic protists (the uptake of particles by eukaryotic cells) (Pernthaler, 2005). Protists can compete with bacteria for DOM and may also feed directly on bacteria. In oligotrophic systems, bacterial concentration

is more tightly controlled by protistan predation, while in more productive waters it is the competition for nutrients which limits their growth.

The Microbial Carbon Pump

The term microbial carbon pump (MCP) (figure 1.4) refers to the microbial processes that transform labile dissolved organic carbon (LDOC) into recalcitrant dissolved organic carbon (RDOC) (Jiao et al., 2010). The MCP concept provides a link between microscale processe and macroscale consequences as RDOC can persist for periods of the order of thousands of years at any depth in the water column, including the surface ocean (Jiao and Zheng, 2011). The transformation of dissolved organic carbon (DOC) is carried out by heterotrophic microbes and the availability of DOC compunds to microbes shapes microbial diversity and community structure (Giovannoni and Stingl, 2005). Different clades will have different responses and thus impacts on the DOC pool in the ocean (Jiao and Zheng, 2011).

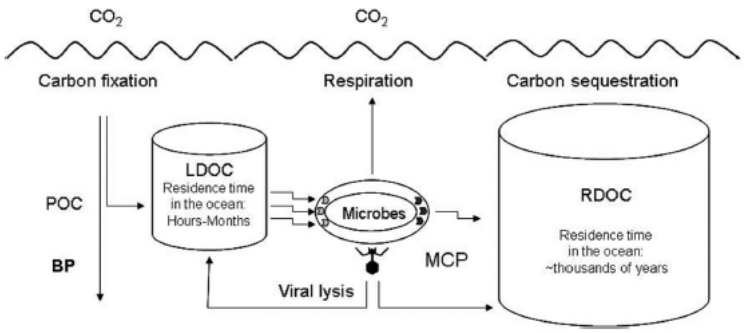

Figure 1.4: The microbial carbon pump (MCP) in the context of carbon cycling in the ocean. This newly proposed mechanism lies upon the theory that microbial processes that transform labile dissolved organic carbon (LDOC) into recalcitrant dissolved organic carbon (RDOC). POC, particulate organic carbon; BP, biological pump (POC sinking to from the surface to depths and even seafloor). (After Jiao and Zheng (2011))

Bacteria can be both consumers and producers of DOC in the ocean. Ogawa et al. (2001) demonstrated that heterotrophic bacteria can take up LDOC even at very low concentrations and generate RDOC very rapidly. Apart from bacterial excretion, another important MCP pathway is viral lysis and some of the lysis productions are resistant to further microbial use.

The production and turnover of RDOC is still poorly quantified (Jiao and Zheng, 2011) and the role of MCP in the world's oceans is yet to be thoroughly understood. A deeper comprehension could slightly change perspectives of the ocean's response to global warming and to the constant increase of CO_2 in the atmosphere.

1.4 The Gulf of Trieste

The Gulf of Trieste is a semi-enclosed basin situated in the north Adriatic Sea bordered by Italy and Slovenia on the east coast and with an average depth of 20m (Figure 1.5). The bathymetry of the Gulf is asymmetrical with depths increasing gently from northern and northwestern coast to the south (Malacic et al., 2006; Solidoro et al., 2007). The maximum depth of ∼25m is found in a narrow area in front of the Istrian Peninsula (Mauri et al., 2008).

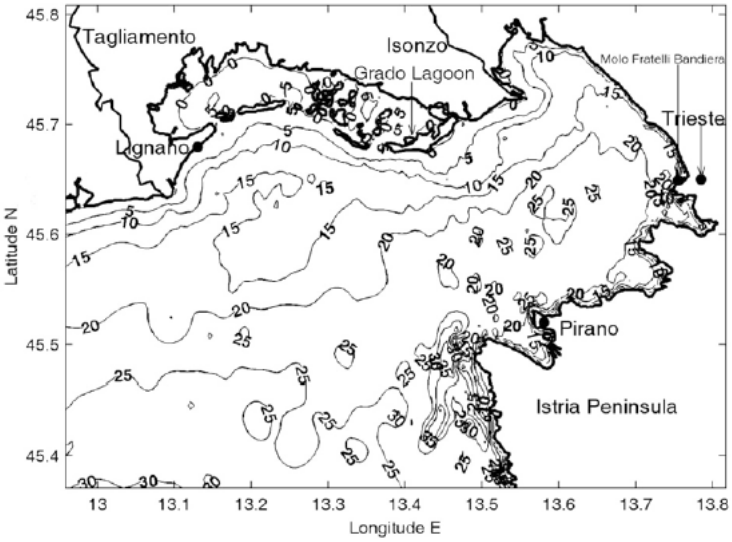

Figure 1.5: Geographical and bathymetrical map of the Gulf of Trieste (After Mauri et al. 2008)

1.4.1 Temperature and salinity structure

In the Gulf of Trieste water temperature variations are up to 16°C between summer and winter. During cold months minimum temperatures are uniform through the water column, while in summer months a thermocline is observed with temperature changes of up to 8°C between the surface and the bottom. During winter, large amplitude wind events cause a decrease in surface temperatures inducing mixing of the water column.

The mean salinity in the gulf is of ∼37.1 psu with the main freshwater source to the Gulf being the Isonzo river on the north-western coast which has an annual average flow rate of 204 m^3s^{-1} (**?**). The contribution of other rivers (Timavo, Ospo) is negligible amounting only to ∼10% of the total runoff. The flow regime of the Isonzo river is generally characterized by low values in early winter and summer and high values in early spring and autumn. The fresh buoyant water coming from the Isonzo is warmer than the surrounding waters and therefore produces stratification and creates large

density gradients.

1.4.2 The circulation

In the northern Adriatic, river runoff plays an important role exceeding evaporation also during summer. This area is known to have a cyclonic circulation, with intensified jets along the western Adriatic coastlines but seasonally varying in strength (North Adriatic Gyre). The Western Adriatic Coastal Current (WACC) is formed by cold and brackish water mainly coming from the Po discharge, and follows the Italian coast due to the Coriolis effect. Its outflow is compensated by the inflow of the Levantine Intermediate Water (LIW). The Gulf of Trieste is subject to the same circulation with LIW entering the Gulf from the South-East and denser water forming due to the Isonzo brackishwater and exiting on the western side. Currents are usually weak and form a cyclonic circulation in the surface layer (3-5m) with speeds ($\sim$5-6 cm s^{-1}) depending on the sea/land breeze (Celio et al., 2006). The bottom layers are usually characterised by a weak cyclonic circulation originating form outside the Gulf.

However, strong wind events form the North-east (Bora) can cause the surface circulation in the Gulf to reverse. In fact, Bora forces the outflow of surface waters and in occasions when the wind is steady, the pressure gradient force balances the wind stress driving the subsurface inflow from the Adriatic Sea to the open sea areas. Wind therefore plays a crucial role for the flushing of the Gulf and the mixing of the water column. Strong wind-driven currents homogenize the water column and can flush the whole basin in almost 3 days (Mauri et al., 2008).

On the other hand, tidal currents (amplitude$\sim$10 cm s^{-1}) do not play an important role for the circulation of the Gulf (Malacic and Viezzoli, 1998). The tidal signal in the northern Adriatic is of mixed type, with the semidiurnal component M2 and diurnal component K1 having comparable amplitudes. Tidal currents move northwards along the eastern Adriatic coast, passes through the Gulf of Trieste reaching maximum amplitudes of 81 cm in Trieste, and then circulates South-westward along the Italian coast.

1.4.3 Biogeochemistry of the Gulf

The coast of the Gulf of Trieste is heavily inhabited and has important harbors and tourist, fishing and aquaculture activities. This anthropogenic influence contributes to the interannual variability of chemical parameters (Mozetic et al., 1998). River inflows and circulation are a major forcingof biogeochemical properties of the area (Solidoro et al., 2007). In the Gulf, nutrient concentrations and consequently biological activity

strongly depend on the Isonzo river discharge which may vary from year to year. Other nutrient contributions to the water column may derive from local precipitation, aerosols and smaller river inputs, but none of these significantly contribute to the total budget.

Generally speaking, the Gulf, as most of the Mediterranean, is P-limited with concentrations ranging from $\sim$0.01 to 0.15 μmol and highest values in October. Allochthonous inputs of phosphate, which range between 0.05 and $>$3 μmol at the surface, are mainly due to sewage input (Fonda Umani et al., 2007). During winter the concentration of phosphate in the Gulf does not appear to be controlled by the river input, but the key role seems to be played by phytoplankton uptake (Zavatarelli et al., 1998). Also, the large amount of semiliable dissolved organic carbon induces a strong bacterial uptake of the limiting nutrient, limiting phytoplankton growth (Polimene et al., 2007).

The annual cycle of phytoplankton in the system is characterised by an intense late winter diatom bloom, a nutrient-depleted summer and a second short-lasting fall bloom (Mozetic et al., 1998). Strong river inflow in early spring can be reflected in higher nitrate concentrations in the water column. This has a direct effect on phytoplankton abundance which normally sees a strong rise in this period due to the intense growth of diatoms (Cantoni et al., 2003) and an increment of irradiance. Moreover, the increased Isonzo outflow causes a stratification of the water column with brackish and warmer waters on the surface. As spring proceeds, after this initial bloom due to the favourable conditions, diatom abundance falls due to the shortage of silicate and grazing pressure. Also, regeneration of NH_4 occurs in the deeper waters.

During summer, freshwater and nutrient inputs are low. Moreover, the consumption of nutrients during the spring bloom causes a decrease in their concentration and an increase in mineralization. In summer, physical characteristics of the water column are favourable as the irradiance is high and the water column is well stratified. Therefore, although physical conditions are ideal for a bloom in primary production, nutrient depletion limits their growth. During late summer and autumn, ammonium and silicate concentrations are low in the upper layers and maximum just above the bottom. In this period bacterial mediated remineralization of organic matter, and the heterotrophic part of the microbial food web (the microbial loop) conveyed most of the energy cycling in the ecosystem (Solidoro et al., 2007).

The autumn peak of freshwater discharge usually occurs in the Gulf of Trieste more regularly than the spring one (Mozetic et al., 1998). This brings new nutrients to the systems which sees a second peak in phytoplankton growth. This peak of primary production determines the reduction of DIN:PO_4 and Si:PO_4 ratios(Cantoni et al., 2003).

Winter waters are characterized by scarce phytoplankton abundance due to the

low irradiance, low temeprature and the mixed water column. During winter period heterotrophic processes prevail favouring the stratification of the water column and enriched nutrients concentration in the euphotic layer (Fonda Umani et al., 2007). Due to the low river input and the photosynthetic activity, pools of dissolved inorganic nutrients are depleted, especially in surface layers. In late autumn and winter, after the second diatom bloom, microbial food web activities and remineralization prevail. In fact, nutrient recycling becomes the most important process to sustain the productivity after riverine input. Moreover, riverine load does not balance the high NH_4 uptake meaning that it has to be balanced in this shallow ecosystem by nitrogen recycling. This means that the behavior of ammonium is mostly determined by biological processes rather than by the physical transport.

In fact, nowadays it is well established that the microbial food web plays a very important role in recycling nutrients and fuelling primary production, and a very common view of marine ecosystem functioning includes a first phase in which most of the energy flows along the traditional food chain (diatoms, grazers, fish), followed by a second phase in which the autotrophic components of the microbial food webs (essentially picoplankton and their grazers) prevail, and by a third moment dominated by the microbial loop (Legendre and Rassoulzadegan, 1995).

The northern Adriatic is also characterized by massive occurances of mucilage which, as De Vittor et al. (2008) shows, partially depends on the malfunctioning of the organic carbon cycling. Dissolved Organic Carbon (DOC) plays an important role in the carbon cycle because it is the largest reservoir of organic carbon in the ocean. Its concentration results from a large array of production, consumption and transformation processes, due to biological activity, in the different layers of the water column (De Vittor et al., 2008).

The bacteria pattern in the Gulf of Trieste is characterized by persistently higher numbers during late spring to autumn in respect to earlier in the year. Bacteria Carbon Production (BCP) instead sees a maxima in August and September, while lower rates occur during winter and spring (Fonda Umani et al., 2007).

1.5 Thesis objectives

The aim of this thesis is to understand the low trophic level ecosystem structure in a typical estuarine Gulf such as the Gulf of Trieste (Italy). In order to do this we will use a numerical model in a "mechanistic" way, i.e. we will modify the trophic interactions in order to demonstrate the importance of the different functional ecosystem components in the organic carbon flux dynamics. Two are the major objectives:

- Investigate the microbial role in the carbon cycling that determines differences between the microbial pathway and the herbivore pathway
- Investigate the competition between plankton and bacteria on nutrients cycling and comprehend the major role of bacteria: competitor or recycler?

The numerical model used in the thesis is a 1-D version of the Princeton Ocean Model (POM) coupled to the Biological Flux Model (BFM, http://www.cmcc.it/data-models/models/general-description).

This study is innovative as the contribution of the individual pathways and the role of bacteria in a coastal estuarine circulation area has seldomnly been discussed. The mechanistic methodology enables us to simulate a realistic situation with both phytoplankton and bacteria considered, and then to eliminate the bacterial loop and quantify the differences. Moreover, it allows to understand the importance of the competition between bacteria and plankton over dissolved nutrients. This approach has recently been used by Vasseur and McCann (2005) to investigate biological communities response to warming and by De Senerpont Domis et al. (2007) to estimate the effect of different climate warming scenarios on the population dynamics of three algal functional groups.

This insight on the microbial pathway and bacterial competition may reveal important new information on the microbial loop and on the carbon sequestration, and could lead to new implications on the ocean's carbon sequestration in future scenarios.

Chapter 2

Materials and methods

2.1 Observational data set

In this study, new climatologies for temperature, salinity, chlorophyll, oxygen, phosphates and nitrates were calculated from available data sets in the Gulf of Trieste. Only data from year 2000 to present day was considered. Temperature and salinity climatologies were calculated in order to produce initial conditions for the numerical model. Tweleve profiles were therefore calculated by computing monthly means and interpolating them using the uni-dimensional interpolation on the model's grid. The sigma layers of the model are logarithmically distributed near the bottom and surface and the depth for this implementation is of 20m. For the other variables seasonal means were calculated. The data utilized originates from the National Oceanographic Data Center/IOC (http://nodc.ogs.trieste.it/), Massimo Celio (http://www.arpa.fvg.it/) and Vlado Malacic (Malacic et al., 2006).

In order to better represent the Gulf of Trieste, the site of implementation was chosen to be in the middle of the Gulf (station AA1, figure 2.1) where the Isonzo River influence is not too strong. Because of this, of all the data only a small rectangle was considered between 13.4 and 13.7°E, and 45.6 and 45.72°N. A depth criterium has also been applied to all data extractions, and casts with a bottom depth off the range H $\pm$ 5 m have been rejected. Once all data from years previous to 2000 and outside the selected rectagle was removed, the statistics was applied to it.

Seasonal means were calculated for the above mentioned variables. Seasons were divided as follows: winter from January to March, spring from April to June, summer from July to September and autumn from October to December. Contrastingly, following Artegiani et al. (1997a) temperature and salinity seasons were as follows: winter from January to April, spring from May to June, Summer from July to October and autumn from November to December.

Figure 2.1: Location of the station reproduced by the model in the Gulf of Trieste (Northern Adriatic) (modified from Ogrinc et al., 2003)

In order to briefly compare the two climatologies, representations of the temperature Hovmöller plots for ORIG (ABCD.2 dataset) and NEW (calculated recent climatology) are shown in figure 2.2. In ORIG the typical formation and rupture of the thermocline can be observed. March is the month during which the thermocline starts to form before reaching the maximum gradient with an excursion of ∼12°C from surface to bottom in June. Maximum temperature of ∼27°C in the surface is reached in July. Temperatures on the bottom also see an increase between September and October. In October temperature is clearly inversely distributed due to the sea surface cooling processes. This feature is also detectable in September, November and December. During the cold months, January and February, temperature is uniformly distributed with very small shifts in the water column due to strong mixing. February is the coldest month with an average temperature of ∼7°C.

Temperature profiles of NEW differ quite significantly from those of ORIG especially for the fact that there is a weaker thermocline. April is the first month in which a small gradient can be observed between surface and bottom, and the strongest is reached in June as for ORIG, with an excursion of ∼9°C. Maximum surface temperature of ∼26°C in found in August. In contrast with ORIG, data from the run NEW does not exhibit a strong inverse distribution of temperature, rather a slight one of ∼1°C in October, November and December. Again, the cold months, January, February and March, exhibit a well mixed water column with February being the coldest month with a mean water column temperature of ∼8°C.

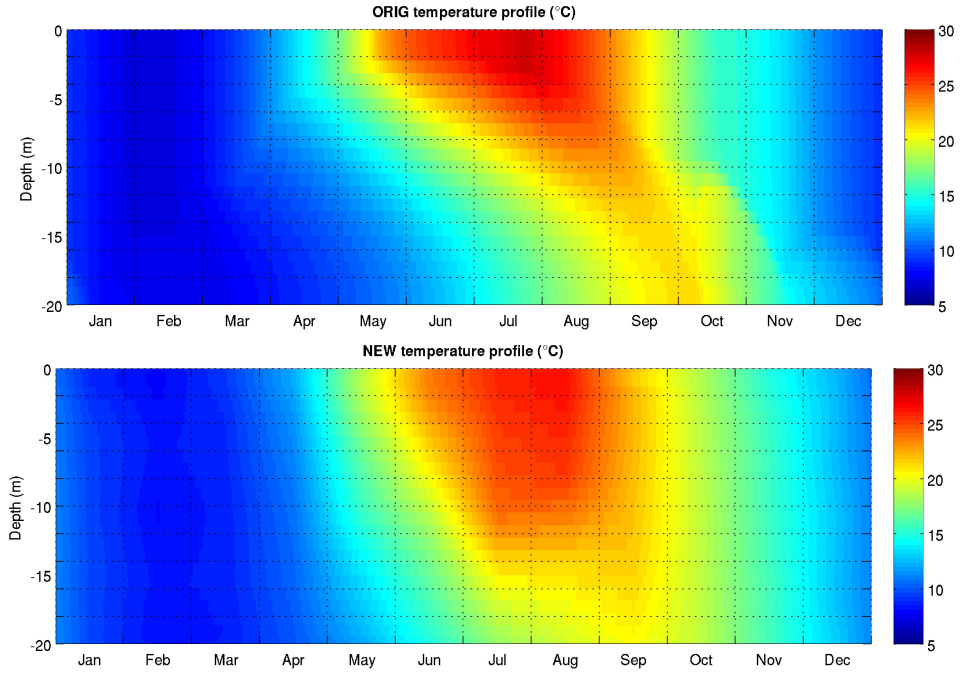

Figure 2.2: Temperature profiles of the model output with original settings (ORIG) and with the new climatology (NEW)

Figure 2.3 represents the salinity Hovmöller plots. Salinity in ORIG sees the largest change between the surface and the bottom from April to July where there is a shift of $\sim$3 psu.

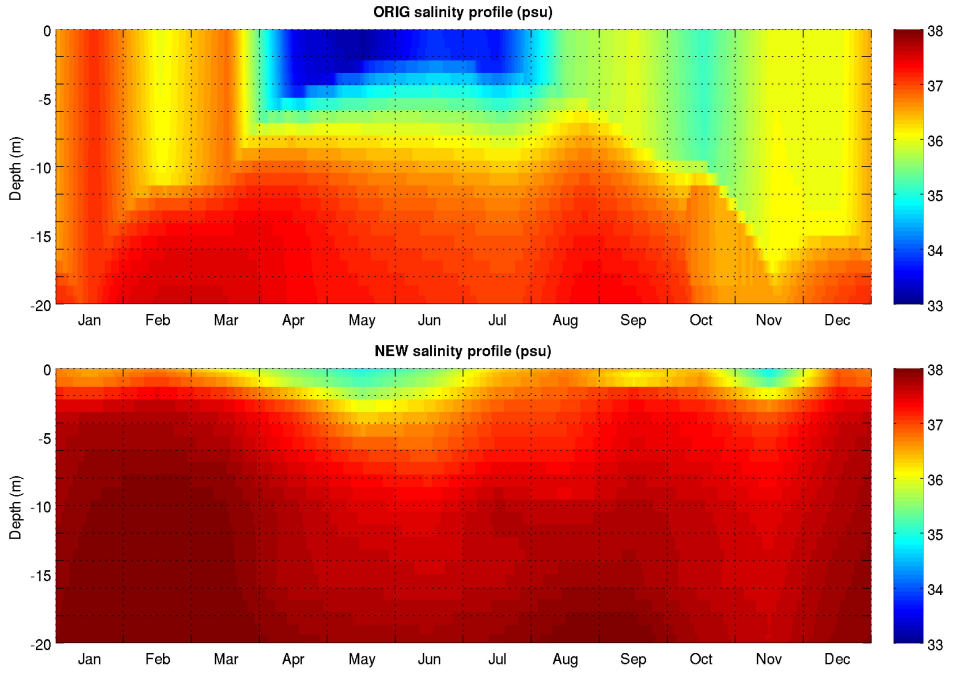

Figure 2.3: salinity Hovmöller plots of the model output with original settings (ORIG) and with the new climatology (NEW)

A halocline is present in October at a depth of ∼10m where salinity rapidly increases of 1 psu. The cold months have a smaller change in the salinity profile and haloclines are detectable from as early as February.

Salinity in NEW shows again some differences from ORIG. The first thing that catches the eye is the much smaller range of salinities throughout the year and the high values. Here the largest vertical change happens in May where salinity varies by 1.8 psu from surface to bottom. However, there is a second period where surface waters see a decrease in salinity and this occurs in November, although this has a smaller shift.

At no stage during the year does a profile look uniform through the water column in contrast with January in ORIG. The dense and heavy bottom water seems to be always present and not influenced by surface brackish waters.

The fact that in the case of NEW, where temperature and salinity climatologies were imposed, the stations close to the coast influenced by river outflow were not considered, could partly explain the differences seen with ORIG. In all plots an abrupt change can be observed on the seafloor in mid-October. A possible explanation for this feature in the benthic layer could be related to the density gradient (figure 2.4) and the mixing of the water column. The abrupt density change could cause mixing of the water column, resulting in this "jump".

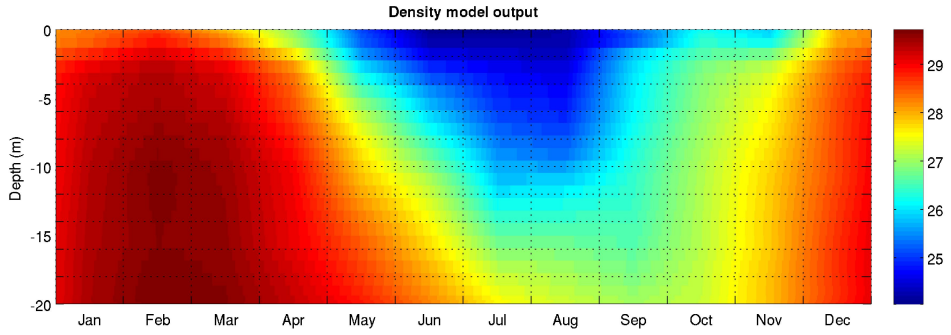

Figure 2.4: Density Hovmöller plot. The abrupt change in density in October and the consequent mixing of the water column cause a step-like feature detectable in most of the plots.

Figure 2.5 represents the chlorophyll seasonal vertical profiles in the Gulf. Surface concentrations are highest during autumn and decrease with depth. The same shape can be seen for winter. Contrastingly, for summer and spring concentrations increase with depth marking the subsurface chlorophyll maximum. In fact, highest chlorophyll concentrations of 2 mgChlm^{-3} are found close to the seabed during summer.

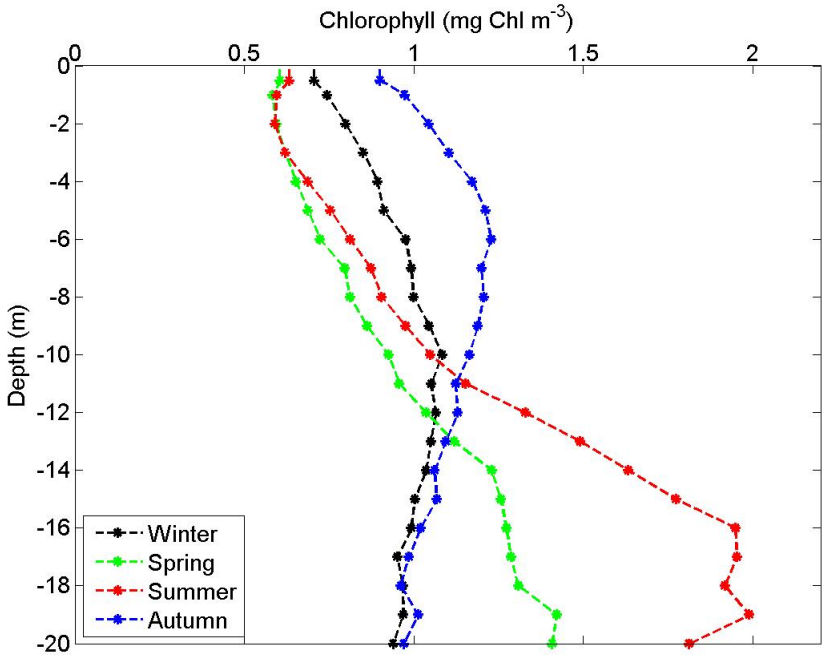

Figure 2.5: Chlorophyll seasonal observations in the Gulf of Trieste comprising of 1202 vertical profiles in the period 2006-2011

The dissolved oxygen seasonal vertical profiles (figure 2.6) show a progressive decrease with depth during winter and autumn, while a subsurface maximum close to the seabed in summer and spring. This behaviour is analogous to the chlorophyll profiles and may occur as a consequence of variations in temperature and the vertical stratification conditions.

Nitrates profiles (figure 2.7) are generally characterised by high surface concentrations due to the influence of the river input, a decrease to about 13m and a small increase in the last section of the water column. During autumn the vertical increase is particularly marked, while in spring this increase is not observed possibly as a consequency of high productivity. The summer profile has generally the lowest concentrations and variation with depth.

The phosphate seasonal cycle differs from the nitrates especially for the fact that summer has the highest concentrations and not the lowest, and because concentrations in the top 10m during winter, spring and autumn exhibit a reduced variability.

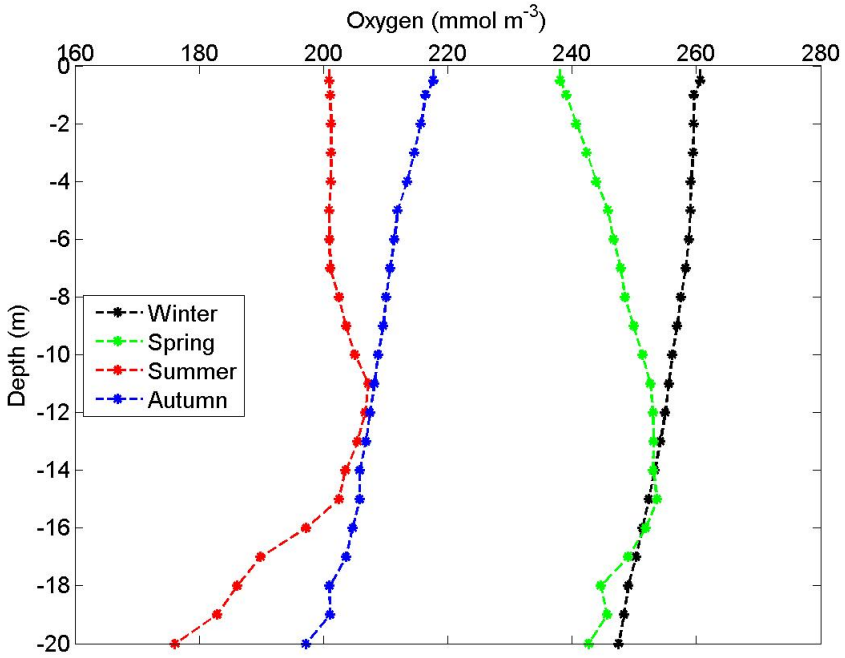

Figure 2.6: Oxygen seasonal observations in the Gulf of Trieste comprising of 1202 vertical profiles in the period 2006-2011

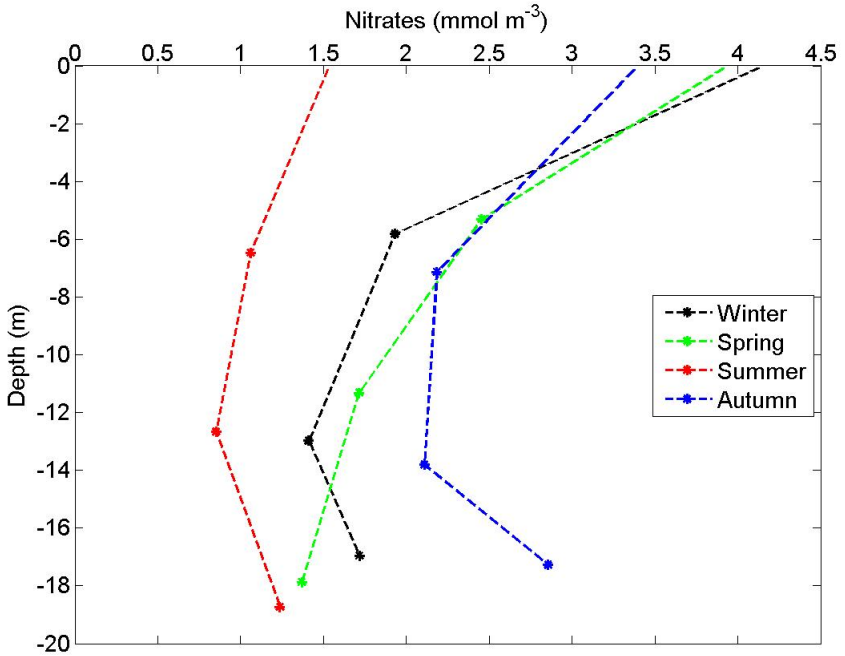

Figure 2.7: Nitrates seasonal observations in the Gulf of Trieste comprising of 439 vertical profiles in the period 2000-2007

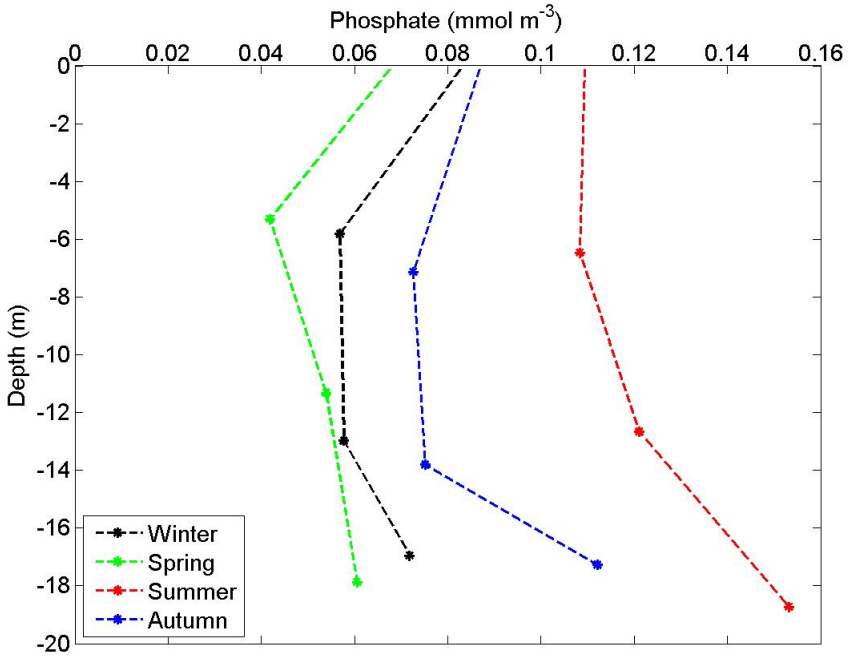

Figure 2.8: Phosphate seasonal observations in the Gulf of Trieste comprising of 431 vertical profiles in the period 2000-2007

2.2 The coupled numerical model

The experiments in this work were carried out using the coupled numerical model resulting from the uni-dimensional version of the Princeton Ocean Model (POM) and the Biogeochemical Flux Model (BFM). The coupling between the two models is schematically represented in figure . At each model timestep (864 seconds), the hydrodynamics computed by POM provides the BFM with information about the physical environment (Vichi et al., 2003). The BFM combines the physics with the biology to compute the temporal rate of change of a generic biogeochemical variable A (expressed in terms of concentration) as follows:

$$\frac{\partial A}{\partial t} = \left.\frac{\partial A}{\partial t}\right|_{phys} + \left.\frac{\partial A}{\partial t}\right|_{bio} \tag{2.2.1}$$

where

$$\left.\frac{\partial A}{\partial t}\right|_{phys} = -\left(w_u + w_s\right)\frac{\partial A}{\partial z} + \frac{\partial}{\partial z}\left[K_H \frac{\partial A}{\partial z}\right] \tag{2.2.2}$$

is the rate of change due to physical processes and $\left.\frac{\partial A}{\partial t}\right|_{bio}$ is the rate of change due to the biogeochemical interactions. In equation 2.2.2, w_s is the settling velocity of the variable and w_u is the vertical advection. For the dissolved constituents,w_u is different from zero only because from a physical point of view there is no difference from water and$w_s = 0$. Diffusion is represented by $\frac{\partial A}{\partial z}$.

Vertical velocity and the diffusion coefficient are fundamental to represent the change in time for the physical part. The physics and the biology share the turbulent coefficients: $\left.\frac{\partial A}{\partial t}\right|_{bio}$ takes light, temperature, salinity and mixing from the physics. The initial conditions for equation 2.2.4 are:

$$A(z)\big|_{t=0} = A_0(z) \tag{2.2.3}$$

where $A_0(z)$ is the initial profile of variable A.

The boundary conditions at the surface ($z = 0$) for (2.2.4) are represented by:

$$K_H \left.\frac{\partial A}{\partial z}\right|_{z=0} = 0$$

In our specific case this will not equal zero and it will change due to the presence of the Isonzo river and depending on the season. On the other hand, boundary conditions at the bottom (z = -H)are:

$$K_H \left.\frac{\partial A}{\partial z}\right|_{z=-H} = 0$$

2.2.1 The Biological Flux Model (BFM)

The biogeochemical model is a biomass-based biogeochemical flux model originally constructed to simulate the dynamical cycling of carbon, oxygen and the macronutrients N, P and Si over the seasonal cycle in temperate marine systems (Vilibic, 2003). BFM consists of an interlinked set of differential equations, describing the biological and chemical processes both in the water column and in the benthic system, as forced by external environmental conditions (light, temperature, water hydrodynamics and allochthonous nutrient sources). The main planktonic functional groups are phytoplankton, bacteria, microzooplankton and mesozooplankton (figure 2.9) . These are then further subdivided into specific functional groups such as diatoms, nanoflagellates, picophytoplankton and dinoflagellates in the case of phytoplankton.

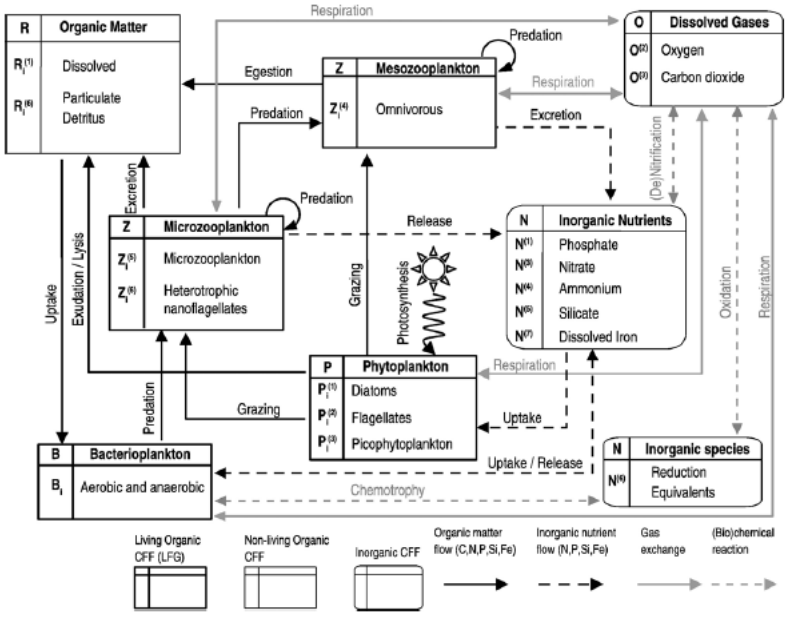

Figure 2.9: Scheme of the state variables and pelagic interactions of the biogeochemical Flux Model (BFM) (After (Vichi et al., 2007))

The model generalizes the biogeochemical concepts developed in ERSEM and adds new important biogeochemical constituents such as iron and chlorophyll. Trophic and chemical interactions in the marine system are represented through the new concept of chemical functional families (CFF) and Living Functional Groups (LFG). CFFs can be sometimes identified as specific compounds such as dissolved inorganic nutrients, but in most of the cases are defined as the inventory of a certain biogeochemical element contained in more complex living and non-living components of marine biogeochemical cycles (Vichi et al., 2007). CFFs are divided into non-living organic, living-organic and inorganic, and are measured based on the major chemical elements (C, N, P, Si, O, Fe)

or on molecular weight units as for chlorophyll (table 2.2). The living organic represent the LFGs which are made up of producers (phytoplankton), consumers (zooplankton) and decomposers (bacteria). The dynamics of each of these are described by population processes (growth, migration, mortality) and physiological processes (photosynthesis, ingestion, respiration, excretion, egestion).

Variable	**Type**	**Components**	**Description**
$N^{(1)}$	IO	P	Phosphate (mmol P m^{-3})
$N^{(3)}$	IO	N	Nitrate (mmol N m^{-3})
$N^{(4)}$	IO	N	Ammonium (mmol N m^{-3})
$N^{(5)}$	IO	Si	Silicate (mmol Si m^{-3})
$N^{(6)}$	IO	R	Reduction equivalents, HS^- (mmol S m^{-3})
$N^{(7)}$	IO	Fe	Dissolved iron (μmol Fe m^{-3})
$O^{(2)}$	IO	O	Dissolved oxygen (mmol O_2 m^{-3})
$O^{(3)}$	IO	C	Carbon dioxide (mg C m^{-3})
$P_i^{(1)}$	LO	C N P Si Fe Chl	Diatoms (mg C m^{-3}, mmol N-P-Si m^{-3}, μmol Fe m^{-3} and mg Chl-a m^{-3})
$P_i^{(2)}$	LO	C N P Fe Chl	Flagellates (“)
$P_i^{(3)}$	LO	C N P Fe Chl	Picophytoplankton (“)
B_i	LO	C N P	Pelagic bacteria (“)
$Z_i^{(4)}$	LO	C N P	Omnivorous mesozooplankton (“)
$Z_i^{(5)}$	LO	C N P	Microzooplankton (“)
$Z_i^{(6)}$	LO	C N P	Heterotrophic Flagellates (“)
$R_i^{(1)}$	NO	C N P	Dissolved organic detritus (“)
$R_i^{(6)}$	NO	C N P Si Fe	Particulate organic detritus (“)

Legend: IO = Inorganic; LO = Living organic; NO = Non-living organic

Table 2.1: List of the chemical Functional Families (CFFs) state variables for the pelagic model (modified from Vichi et al. (2007)) .

Figure 2.10 is a schematic representing the different types of CFFs and the standard organism of the BFM. The standard organism represents the LFGs whose total biomass is composed of living CFFs and interacts with other (living and non-living) CFFs by means of universal physiological and ecological processes (Vichi et al., 2007) mentioned above:

$\frac{dP}{dt}$ = Growth - Exudation - Lysis - Respiration - Grazing

$\frac{dZ}{dt}$ = Ingestion - Egestion - Respiration - Predation

$\frac{dB}{dt}$ = Growth - Remineralization - Respiration - Predation

where P = phytoplankton, Z = zooplankton and B = bacteria.

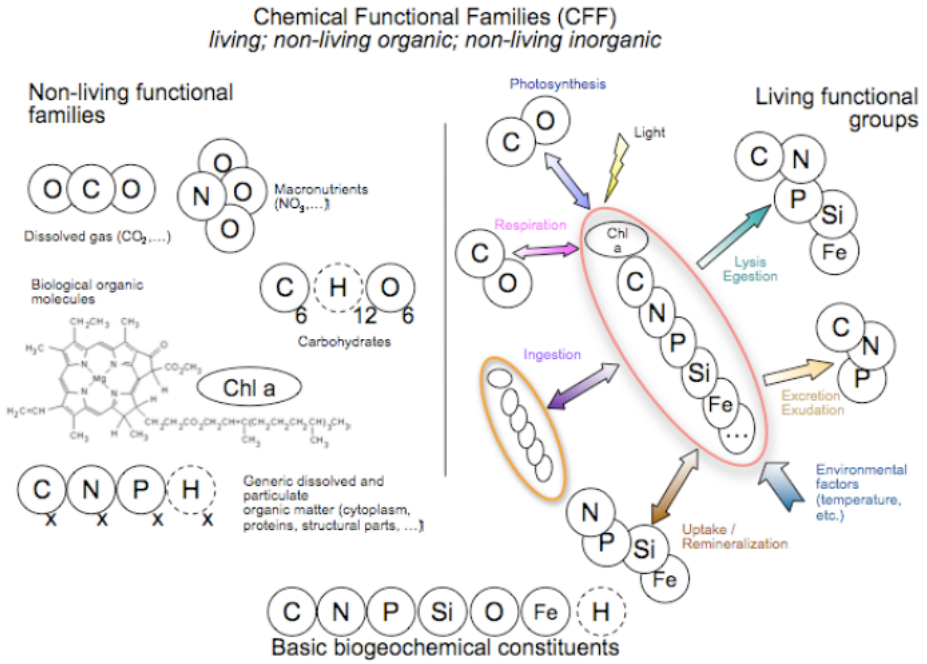

Figure 2.10: Scheme of the various types of Chemical Functional Families (CFFs) expressed in terms of basic biogeochemical elements and of the standard organism of the BFM. In the model, hydrogen is not considered a basic element, but it has been represented in the figure for completeness (After Tedesco and Vichi (2010))

These can be described by the following partial differential equation:

$$\left.\frac{\partial A}{\partial t}\right|_{bio} = \sum_{i=1,nj=1,m} \sum \left.\frac{\partial A}{\partial t}\right|_{V_i}^{e_j} \tag{2.2.4}$$

where the second term describes all the processes of each living and non-living CFF. The superscripts e_j are the abbreviations indicating the process which determines variation (table (2.2.4)), while the subscripts V_i is the CFF state variable involved in the process.

Abbreviations (e_i)	Description
gpp	Gross primary production
rsp	Respiration
prd	Predation
rel	Biological release: egestion, excretion
exu	Exudation
lys	Lysis
syn	Biogeochemical synthesis
nit/denit	Nitrification, denitrification
scv	Scavenging
rmn	Biogeochemical remineralization
upt	Uptake

Table 2.2: List of all abbreviations used to indicate the physiological and ecological processes in Eq.

In the model, hydrogen is not considered a basic element, but it has been represented in the figure for completeness.

At the water sediment interface, a simple benthic closure model was applied, that returns a fixed quota of deposed organic matter as nutrients to the water column to parametrise benthic remineralisation (Butenschon et al., 2012).

2.2.2 The physical model (Princeton Ocean Model)

The Princeton Ocean Model (POM) is a free surface, primitive equation, finite difference model (Blumberg and Mellor, 1983). The 1-D version computes the tracers, temperature and salinity, the velocity components and the vertical viscosity and diffusivity profiles (Bianchi et al., 2006). The basic equations are cast in a bottom following, sigma coordinate system (figure 2.11). The model uses 30 σ levels, where $\sigma = (z-\eta)/(H+\eta)$ for the 3-D version and $\sigma = z/H$ for the 1-D version since in this case the free surface elevation (η) is null; $H(x, y)$ is the bottom topography. Thus, σ ranges from $\sigma = 0$ at $z = \eta$ to $\sigma = -1$ at $z = H$.

POM solves the following 1-D equations:

$$\frac{\partial u}{\partial t} - fv = \frac{\partial}{\partial z}\left(K_H \frac{\partial u}{\partial z}\right) \tag{2.2.5}$$

$$\frac{\partial v}{\partial t} + fu = \frac{\partial}{\partial z}\left(K_H \frac{\partial v}{\partial z}\right) \tag{2.2.6}$$

$$\frac{\partial p}{\partial z} = -\rho g \tag{2.2.7}$$

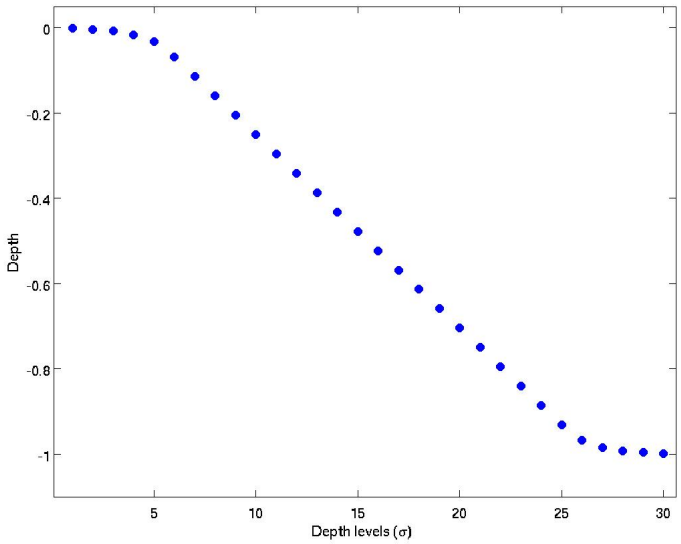

Figure 2.11: Model levels distribution in 20m depth

$$\frac{\partial T}{\partial t} = \frac{\partial I}{\partial z} + \frac{\partial}{\partial z}\left(K_H \frac{\partial T}{\partial z}\right) + \omega_T \tag{2.2.8}$$

$$\frac{\partial S}{\partial t} = \frac{\partial}{\partial z}\left(K_H \frac{\partial S}{\partial z}\right) + \omega_S \tag{2.2.9}$$

The vertical diffusivity coefficients are calculated assuming the closure hypothesis $K_H(z) = qlS_H$ where S_H is an empirical function (Mellor and Yamada, 1982).

$$\frac{\partial}{\partial t}\left(\frac{q^2}{2}\right) = \frac{\partial}{\partial z}\left(K_q \frac{\partial q^2/2}{\partial z}\right) + P_s + P_b - \varepsilon \tag{2.2.10}$$

Equation 2.2.10 defines the change in time of turbulent kinetic energy, $q^2/2$, due to diffusion (K_b), turbulent kinetic energy production by shear (Ps), the buoyant production/dissipation (P_b), and the dissipation due to turbulence (ε). The mixing length is then defined as:

$$\frac{\partial}{\partial t}\left(q^2 l\right) = \frac{\partial}{\partial z}\left(K_b \frac{\partial q^2 l}{\partial z}\right) + E_1\left[P_s + P_b\right] - \frac{q^3}{B_1}\tilde{W} \tag{2.2.11}$$

where $\tilde{W}$ is a function of the distance between rigid boundaries, and E_1 and B_1 are empirical constants.

For the closing hypothesis the equations need specific conditions for the initial condition and the vertical conditions (surface and bottom boundary conditions). The boundary conditions for turbulent kinetic energy at the surface depend on the wind stress intensity (at z=0) and is represented by the semi-empirical equation:

$$q^2 = B_1^{\frac{2}{3}} \frac{|\vec{\tau}_w|}{C_d} \tag{2.2.12}$$

where $\vec{\tau}_w = C_d \bar{U}_{wind} \left|\bar{U}_{wind}\right|$ is the wind stress at the surface, C_d is the surface drag coefficient, $\bar{U}_{wind}$ is the horizontal wind velocity at the surface.

Top and bottom boundary conditions

Wind gives a strong energy input and is given by wind waves which break. When they break, there is a transfer of energy to turbulence which gives a coefficient and results in a current:

$$K_M \frac{\partial \vec{u}}{\partial z}\bigg|_{z=0} = \vec{\tau}_w \tag{2.2.13}$$

where the x-component is $\tau^{(x)} = C_d \left|\vec{u}_w\right| u_w$, the y-component is $\tau^{(y)} = C_d \left|\vec{u}_w\right| v_w$ and $\vec{u}_w = (u_w, v_w)$.

$$K_H \frac{\partial S}{\partial z}\bigg|_{z=0} = S_0 \left(E - P - R\right) \tag{2.2.14}$$

$$I = I_0 \left[e^{-\lambda_1 z} R_1 + e^{-\lambda_2 z} R_2\right] \tag{2.2.15}$$

where λ_1 is the attenuation coefficient and $I\left(z\right) = I_0\left(490nm\right) e^{-k_{490} z}$. In the model $K_{490} = K_w + \left(\frac{\partial K}{\partial C}\right) Chl + K_b$.

The bottom is

$$\vec{\tau}_b = C_b \bar{U}\left(-H, t\right) \left|\bar{U}\left(-H, t\right)\right|$$

Here C_b is the bottom drag coefficient and $\bar{U}\left(-H, t\right)$ is the horizontal velocity at the bottom (Bianchi et al., 2006).

2.3 Model set up

POM1D-BFM has previously been validated and tuned in various scientific papers (Zavatarelli et al., 1998, 2000; Polimene et al., 2006a; Vichi et al., 2003).

The wind stress forcing function (τ) used to evaluate boundary conditions, the heat flux terms and the short-wave incoming radiation flux were all calculated from the 6-hours surface reanalyses of meteorological parameters from the European Centre for Medium-range Weather Forecast (ECMWF) for the period 1982-93 (Vichi et al., 2003). The wind stress is also used to calculate the coefficient of diffusion for the

biogeochemical variables, together with temperature, salinity and density. Temperature and salinity monthly mean vertical profiles calculated from observations are forced in the model, which then interpolates them.

The surface fluxes are computed following the procedures described in Maggiore et al. (1998) and Zavatarelli et al. (2002). Inorganic suspended matter seasonal mean concentration profiles in the water column were calculated from observations collected monthly over the period 1997-2000. Perpetual time series of nutrients at the surface are climatological mean seasonal values extracted from the Marine Biology Laboratory (LBM) of Trieste dataset (Vichi et al., 2003).

Detailed representation of the bacterioplankton dynamics related to DOM utilization are implemented: bacterioplankton functional processes include the concept of refractory organic matter. The degree of refractoriness is determined by the carbon/nutrient ratios of DOM and regulate the bacterial uptake of organic substrate (Vichi et al., 2003). Optimal uptake is achieved when the C:N:P ratios in DOM and in bacterioplankton correspond to the optimal intracellular bacterial ratio of 45:9:1 (in atoms, Goldman et al., 1987). The bacterioplankton uptake on dissolved and particulate detritus is defined on the basis of C:N and C:P ratios in DOM and POM, and on the "characteristic" time scales for the uptake process. Also, bacteria are allowed to take-up inorganic nutrients directly from the waters, according to their internal needs (Zweifel et al., 1993).

Since POM1D-BFM is a very complex model where energy has various paths to move through, the aim was to simplify the model in order to understand the energy implemented in different passages and test its sensibility. The first step to achieve this (experiment 1) is to eliminate bacteria from the system and setting them as implicit like for a classical NPZD (Nutrients-Phytoplankton-Zooplankton-Detritus) model. Table (2.3) shows the pelagic remineralization rates in the base experiment for the different organic matter compartments. In a classical NPZD model there is with a unique closure remineralization rate, therefore for our experiments a single value is set for

Symbol	Value (d^{-1})	Description
R6O3	0.1	Remineralization from POM to CO_2
R6N1	0.1	Remineralization from POM to phosphate
R6N4	0.1	Remineralization from POM to ammonium
R1O3	1	Remineralization from DOM to CO_2
R1N1	1	Remineralization from DOM to phosphate
R1N4	1	Remineralization from DOM to ammonium
R2O3	0.1	Remineralization from SLOM to CO_2

Table 2.3: Remineralization values and their description

all compartments. Various values are tested to investigate the model sensitivity, as well as a null closure remineralization (experiment 1a). In a simple normal NPZD model, setting the closure remineralization to a null value causes the model to become unstable, therefore here we test if it is the same case for our model.

The second experiment aims at keeping only the herbivore chain active in the system and in order to do this, all micro components are excluded (bacteria, microzooplankton, picophytoplankton). This removes definitely the remineralization taking place through the microbial compartment and further simplifies the model towards an NPZD model. Table (2.4) summarises the above described experiments.

Experiment	**B**	**Microzoo**	**Picophyto**	**Remin. closure**
Base	✔	✔	✔	✔
Exp. 1		✔	✔	✔
Exp. 1a		✔	✔	
Exp. 2				✔

Legend: B=bacteria; Microzoo=microzooplankton;
Picophyto=picophytoplankton; Remin. closure = remineralization closure;

Table 2.4: Summary of experiments carried out

Chapter 3

Results

3.1 Base experiment and validation of seasonal model results

The base experiment has been initialized with the settings described in chapter 2. A simplified schematic of the model fluxes is represented in figure 3.1. Phytoplankton feeds on nutrients before turning into detritus either directly through sinking or via the zooplankton community (micro- and mesozooplankton) which feeds on it. Microzooplankton also have a function of remineralization which returns nutrients back to the system via excretion.

Similarly to phytoplankton, microzooplankton either die and move to the detritus compartment in the water column, or are fed on by mesozooplankton.

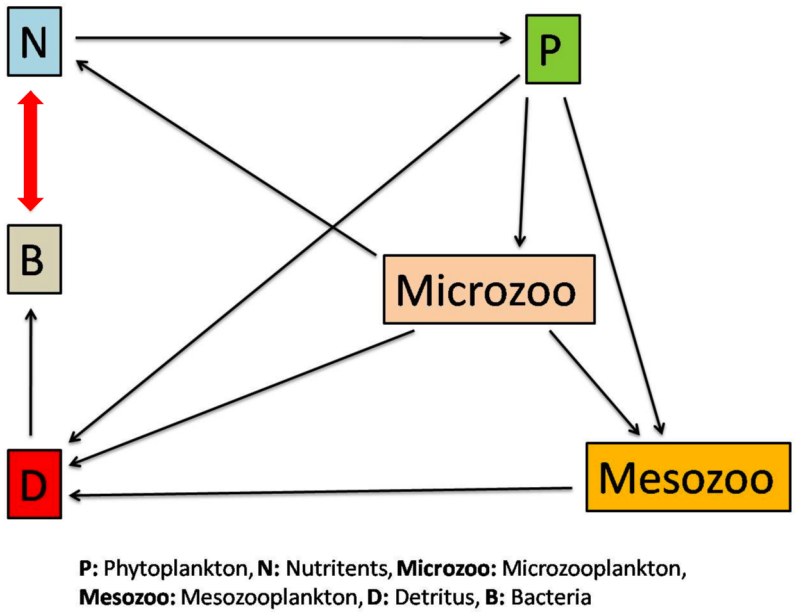

Figure 3.1: A simplified schematic of the model fluxes

Mesozooplankton, on the other hand, predate on phytoplankton and microzooplankton and then convert directly into detritus. Detritus is mediated through bacteria and turned back into available nutrients in the water column. However, as the doublearrow suggests, bacteria may also compete for the nutrients, playing a dual role in the system: source and sink.

Here we validate the base experiment against observations. The latter are seasonal mean vertical profiles of selected variables which will be compared with the corresponding climatological data, as already proposed in Vichi et al. (1998a,b). The data sets described in section 2.1 were used covering the period 2000-present. The seasonal means of model state variables have been plotted against the means and standard deviations of the available observations in the data sets.

Looking at the biogeochemical pelagic variables, figure 3.2 commpares the chlorophyll model output with the *in situ* observations. The two seem to disagree on the position of the subsurface chlorophyll maximum (SCM) in spring and summer. The observations suggest an increase in concentration closer to the seabed compared to the model's output during this period. Also, during winter the model exaggerates the surface chlorophyll concentration while during autumn concentrations in the lower half of the water column seem to be somewhat low compared to the mean seasonal profile. The major error however is the reproduction of the seasonal SCM which is less abrupt in the observed data and closer to the seafloor. Phosphate seasonal concentrations from observations and the model are compared in figure 3.3.

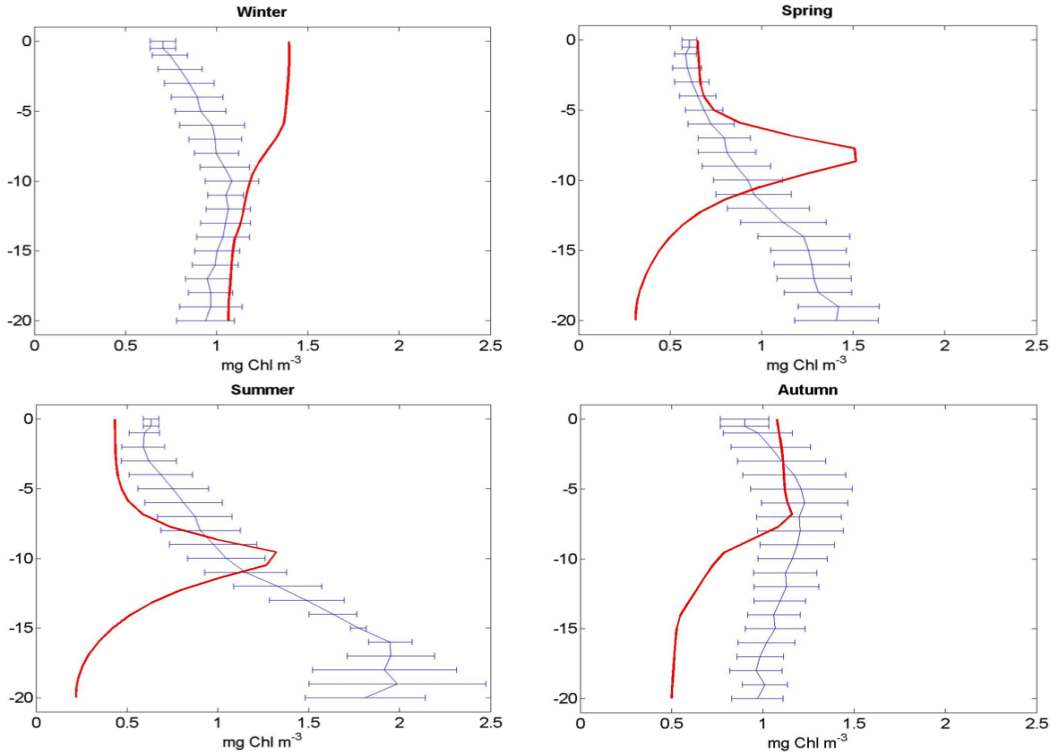

Figure 3.2: A comparison of seasonal chlorophyll concentrations calculated from observations (1202 vertical profiles) with standard deviations (blue) and from the base experiment model output (red)

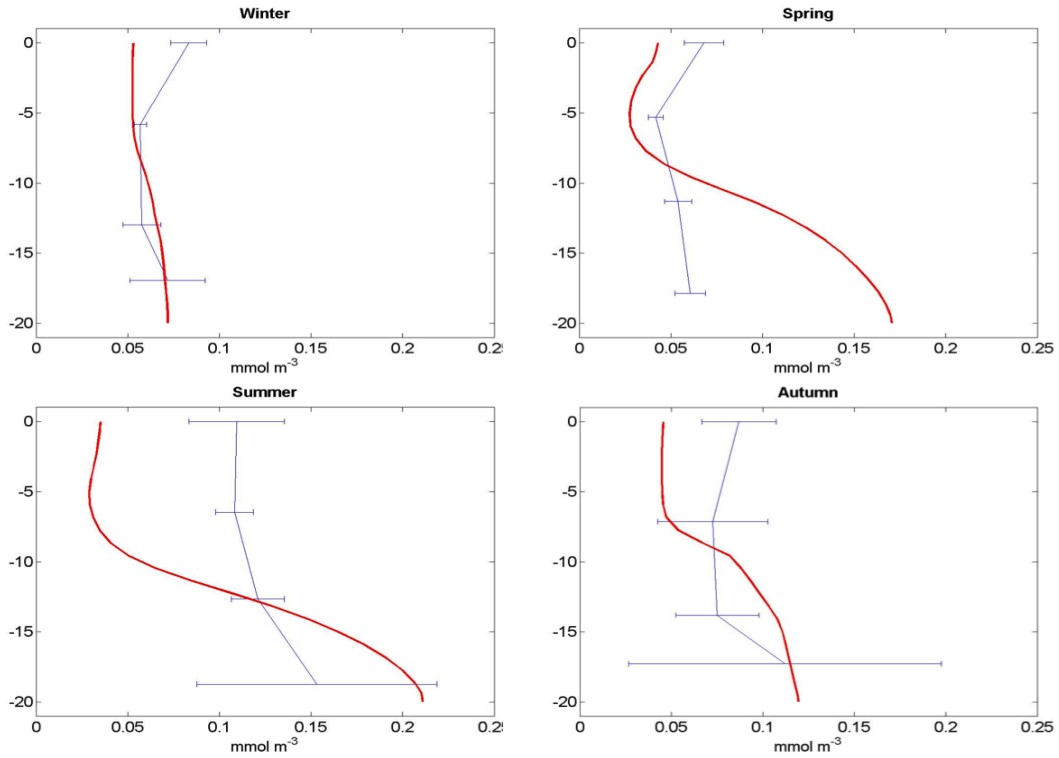

Figure 3.3: A comparison of seasonal phosphate concentrations calculated from observations (431 vertical profiles) with standard deviations (blue) and from the base experiment model output (red)

The model reproduces phosphate in lower concentrations than the observations at the surface during all seasons and in higher concentrations in the subsurface. This difference could be associated to the influence of the Isonzo river waters which have not been correctly set in our simulation. Furthermore, during spring and summer the model seems to exaggerate the vertical nutricline.

Regarding nitrates, the model has a serious problem reproducing the concentrations throughout the water column. This can be seen in figure 3.4 where again, seasonal profiles are compared to the output of the model. In fact, in summer the model in unable to reprodue the profile at all and shows much higher concentrations in respect to the observations. Although summer is the season where this difference is most obvious, the inability of the model to reproduce the vertical profiles is evident during the other seasons too, especially in the lower part of the water column where the model always has much higher concentrations than real conditions.

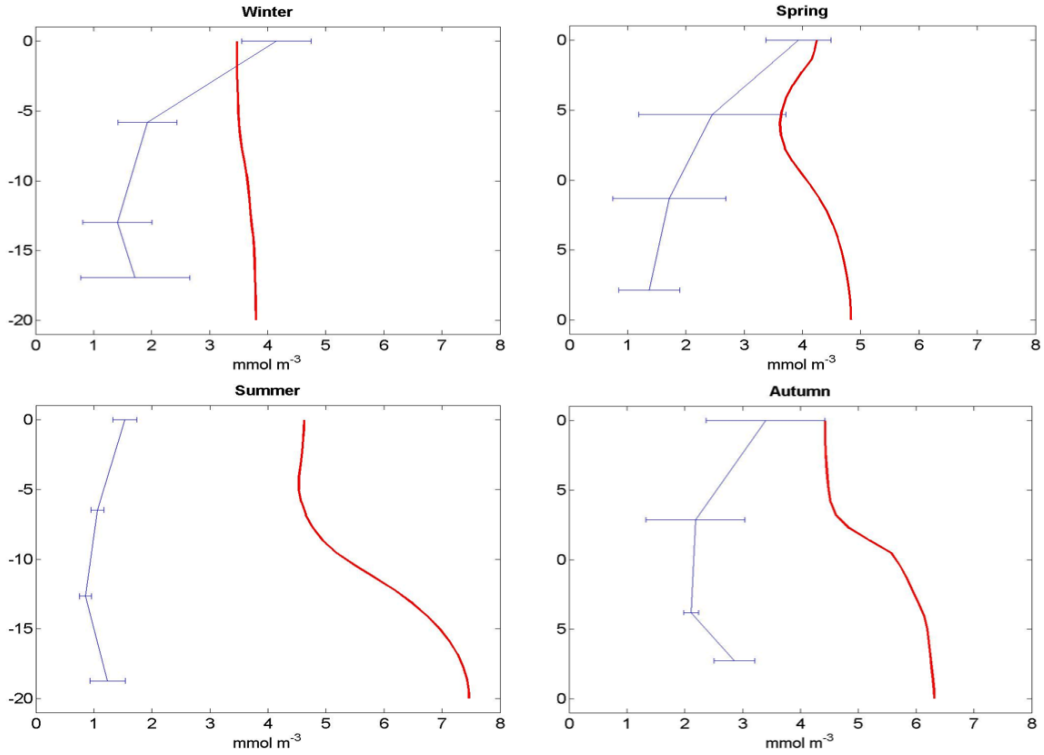

Figure 3.4: A comparison of seasonal nitrates concentrations calculated from observations (439 vertical profiles) with standard deviations (blue) and from the base experiment model output (red)

Finally, the model predictions for oxygen concentrations show smaller differences compared to nitrates (figure 3.5). The model reproduces the winter profile extremally well, however for all other seasons it computes concentrations too low in the bottom half of the water column. In fact, during spring and summer the model shows a completely opposite curve to the real data in this area. In autumn the model shows the strongest oxycline, however observed concentrations decrease gradually and linearly with depth, and do not present an oxycline.

Figure 3.6 represents the Hovmöller plots of the base experiment for phosphate, nitrate and ammonia (note the difference in scale). Phosphate has the lowest concentration and peaks on the seafloor, especially from June to October. Nitrate also see highest concentrations on the seafloor but extending higher, to about 8-10m depth from June to the first half od December. Ammonia peaks in concentration a little earlier in the year, between the second half of March and July and also extends up to about 8-10m depth from the seafloor. A minimum concentration can be seen in all plots during March, from the surface to 8-10m depth which can be understood by looking at chlorophyll distributions below.

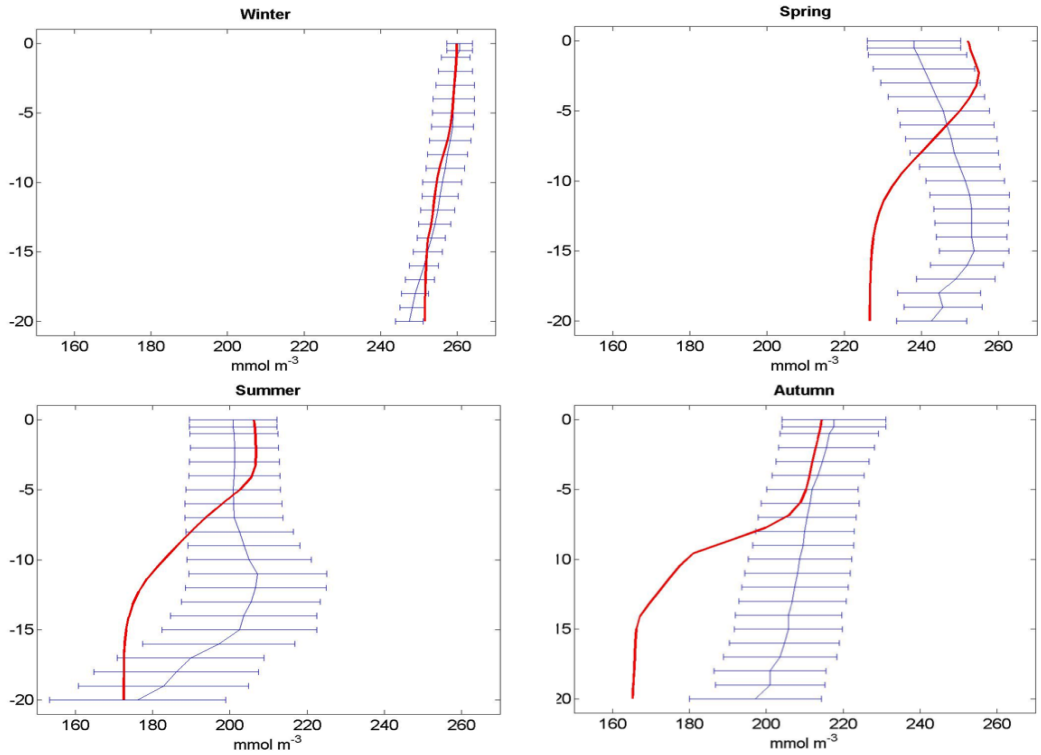

Figure 3.5: A comparison of seasonal oxygen concentrations calculated from observations (1202 vertical profiles) with standard deviations (blue) and from the base experiment model output (red)

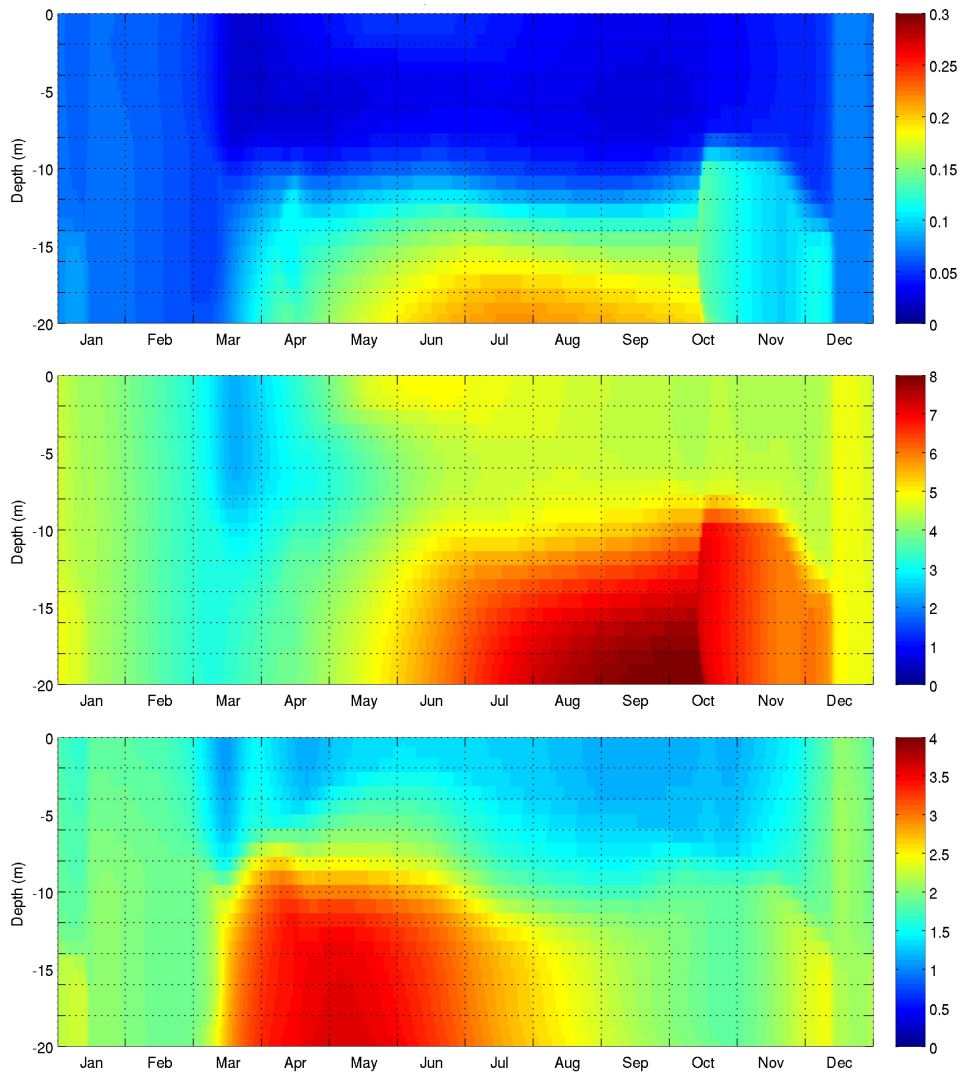

Figure 3.6: From the top, hovmöller plots of phosphate, nitrate and ammonia for the base experiment in mmol m^{-3} (note the difference in scale).

For phytoplankton groups distribution, for which no observational data is available, figure 3.7 shows how most of the chlorophyll derives from the diatoms, the leading phytoplankton group in most coastal marine systems. In fact, it shows how the SCM comprises mainly of diatoms as they bloom in the spring-summer period. During the rest of the year, especially from December to the first half of March, the diatom concentration is more or less stable and equally distributed in the water column thanks to the winter mixing. Lowest diatom concentrations are observed on the surface, in the top 6 meters of the water column during the SCM.

Chlorophyll concentrations in nanoflagellates and picophytoplankton are much inferior, however they both show higher concentrations in March. Therefore, the bloom observed in figure 3.7 in this period is due to these two smaller phytoplankton groups.

Apart from the winter period during which the watercolumn is well mixed, concentrations persist being very low in the benthic area. Nanoflagellate concentrations on the surface remain high for a longer period of time in respect to picophytoplankton. High concentrations of picophytoplankton and nanoflagellates occur in correspondance to lower diatom concentrations.

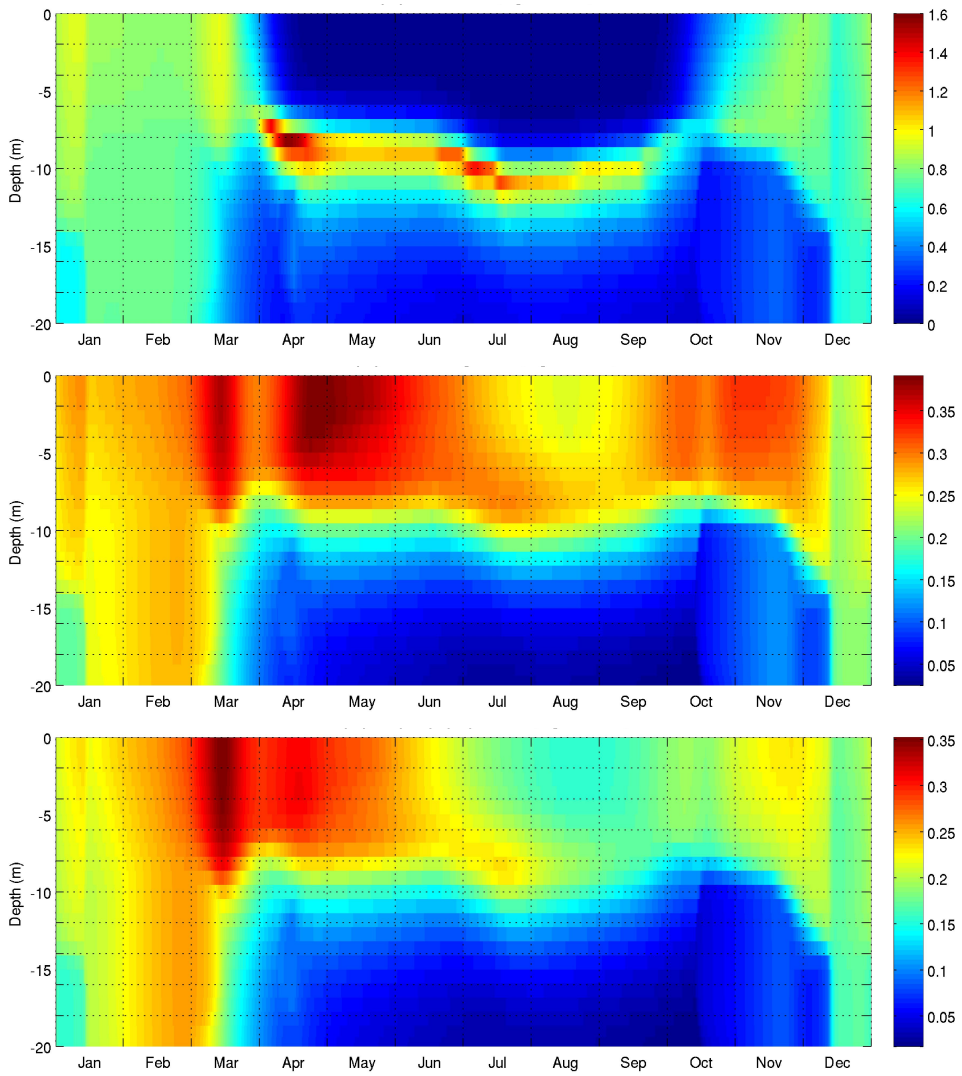

Figure 3.7: Chlorophyll concentrations in diatoms, nanoflaggelates and picophytoplankton from top to bottom for the base experiment in mg Chl m^{-3} (note the difference in scale).

Carbon concentration in bacteria is shown in figure 3.8. Bacteria bloom between March and June in the top half of the water column, in concomitance with low nutrient concentrations and the bloom of nanoflagellates and picophytoplankton. In other words, the smaller organisms prevail in this area and in this period of the year.

Total carbon detritus is shown in figure 3.9. As one would expect, June, July and August are the months with the surface highest values as a consequence of primary production. After the spring bloom, detritus increases and is mainly composed of semi-liable organic matter. The dissolved organic matter (DOM) contribution to the total detritus concentration is only minimal and on the surface. In contrast, although also particulate organic matter (POM) concentrations are very small, high values are closer to the seabed as one would expect being heavier and therefore sinking.

These results highlight how the model is able to reproduce reality only marginally. However, taken this into consideration, the model is used in a qualitative manner rather than quantitative and our interest focuses on the changes the different experiments will show from the base experiment.

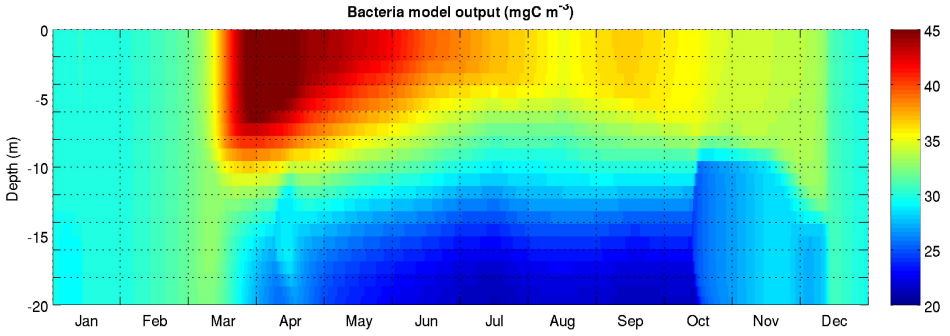

Figure 3.8: Carbon concentration in bacteria for the base experiment in mgC m^{-3}.

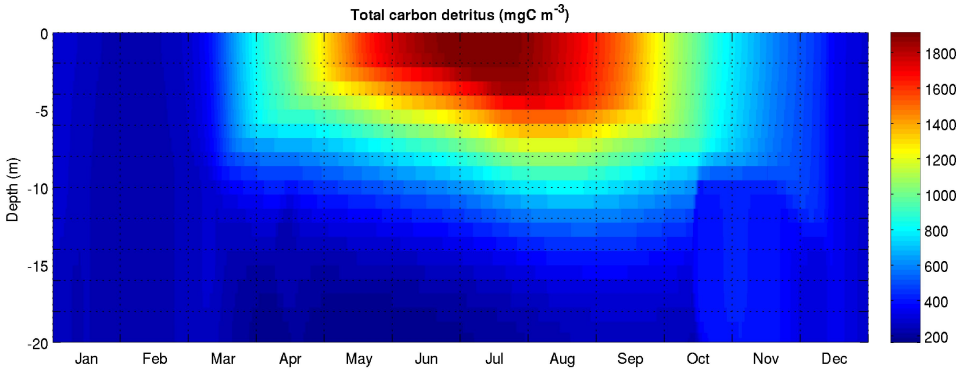

Figure 3.9: Total carbon detritus concentration for the base experiment in mgC m^{-3}.

3.2 Experiment 1 - Eliminating bacteria and testing the model sensitivity to closure parametrizations

Experiment 1 considers no bacteria leaving a remineralization parametrization typical of a simple NPZD model (figure 3.10).

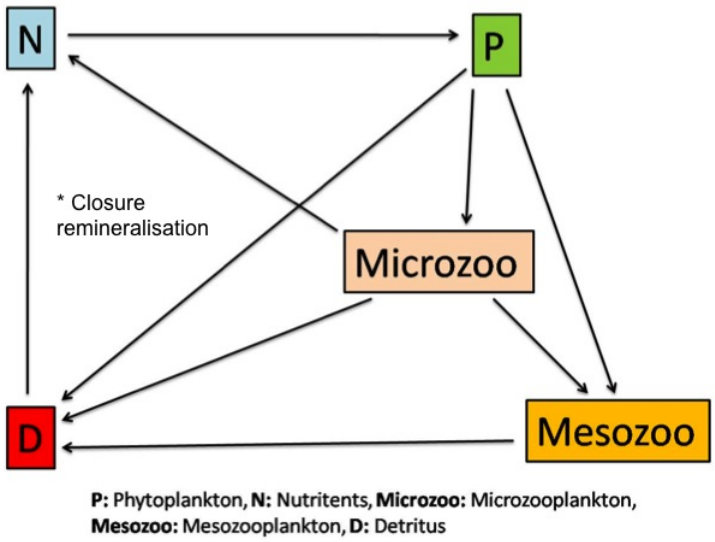

Figure 3.10: Simplified schematic of the fluxes of the model without bacteria in the system

The closure remineralization rates in the base experiment are shown in table (?????). The other values used to test the model sensitivity to closure parametrizations were taken from literature. Fennel et al. (2001) and Kriest et al. (2010) used a remineralization rate of 0.05 d^{-1}, while Spitz et al. (2003) and Powell et al. (2006) used 1.03 d^{-1}. Schartau et al. (2001) used the values 1.12 d^{-1} and 0.69 d^{-1} for two different experiments, whilst Lima et al. (2002) used 0.25 d^{-1}. This large window of closure remineralizations suggested to test the model sensitivity by using the following rates: 0.05, 0.1, 0.25, 0.5, 0.75 and 1 d^{-1}.

The sensitivity of the model will be analysed by comparing results to the base experiment and looking at changes firstly in plankton biomass, secondly in the plankton community and lastly in nutrients concentrations.

Phytoplankton biomass

Figure 3.11 shows results for the total carbon concentration in phytoplankton with increasing remineralization rate. The distribution does not show large differences for closure remineralization rates above 0.25 d^{-1}, therefore it was chosen to show only results up to this remineralization value. The base experiment shows much lower

concentration than any of the other experiments with a clear SCM from April to September. Also, the base experiment shows peak concentrations of both carbon and chlorophyll (figure 3.12) in the surface layer during March and during November. For the other experiments, carbon abundance, which represents biomass, increases as the remineralization rate rises. At the low remineralisation rate of 0.05 d^{-1}, a peak can be seen in March in the top 8 meters and in April between 6 and 8m, mimiking the beginning the SCM. From May to October the water column seems to be vertically divided with average carbon concentrations in the top 10 meters, and very low values in the bottom half. In fact, lowest values occur in the lower half of the water column from March to December. However, between October and November concentrations increase in the top 8 meters marking the autumn bloom. During the rest of the year, from December to February, the water column is well mixed and carbon concentrations uniformly distributed.

With increasing remineralization, both peaks increase in concentration, however the SCM, which is clear in the base experiment, does not develop. In contrast, the spring bloom elongates lasting longer, from March to June, but shallowing in May and June. The autumn bloom also sees a boom with concentrations increasing and its duration slightly prolungated. Moreover, the increase in remineralization causes a very small bloom in the surface waters during the first half of January.

Total chlorophyll concentrations (figure 3.12) exhibit a slightly decreasing trend with increasing remineralization. This contrast with carbon concentrations indicates that although plankton biomass increases with more regenerated production available, production does not necessarily follow this trend. In fact, it is probable that in these conditions with more nutrients available, phytoplankton requires less chlorophyll for growth and this could explain the observed decrease. In any case, concentrations are still all higher than in the base experiment.

The base experiment showed that the chlorophyll distribution was mainly driven by diatoms concentration. Now we will investigate if and how this has changed with the removal of bacteria, and how the result changes with increasing remineralization.

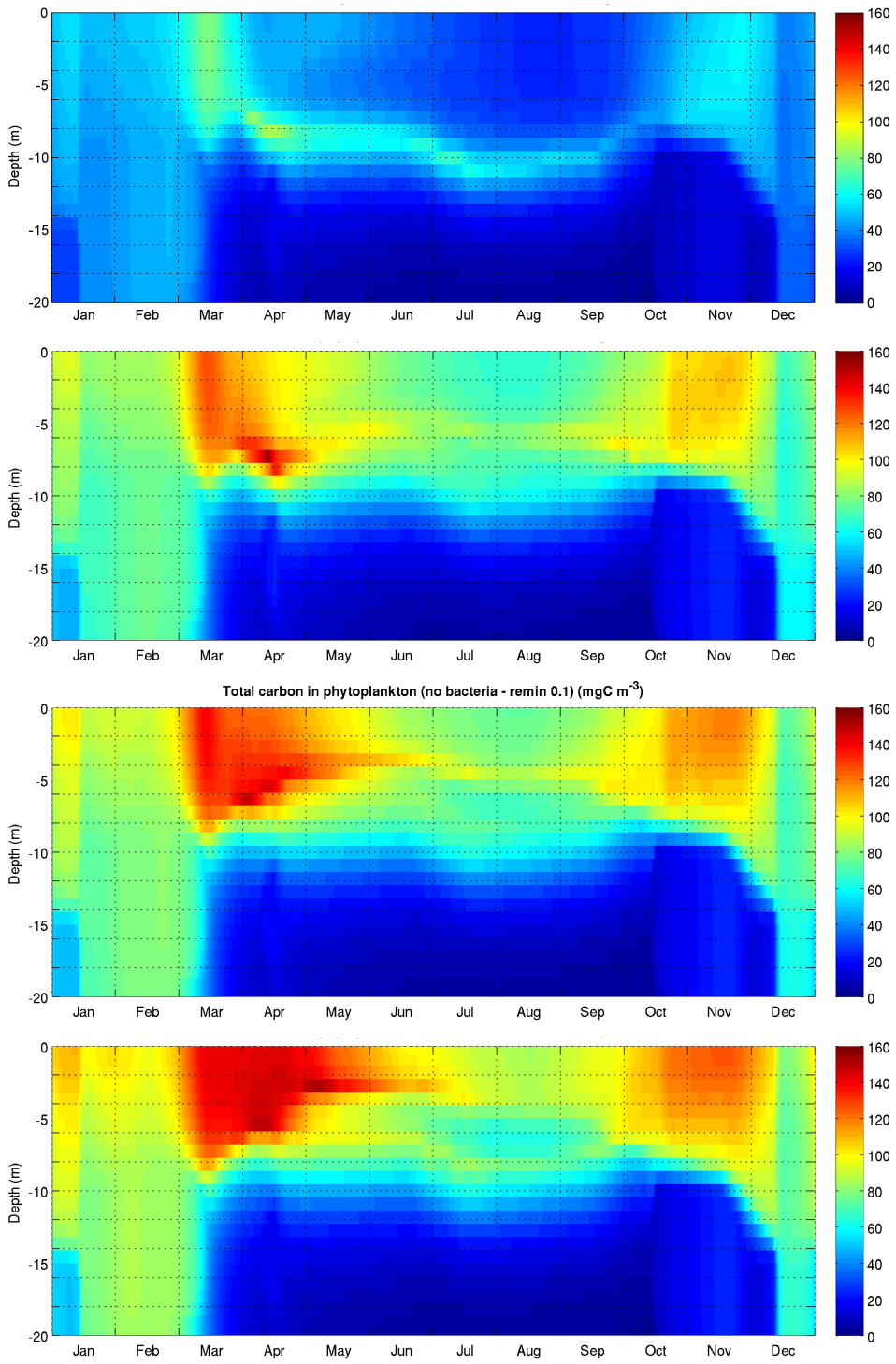

Figure 3.11: Total carbon concentrations in phytoplankton for the base experiment and runs without bacteria and closure remineralization rates of 0.05, 0.1 and 0.25 d^{-1} from top to bottom in mgC m^{-3}.

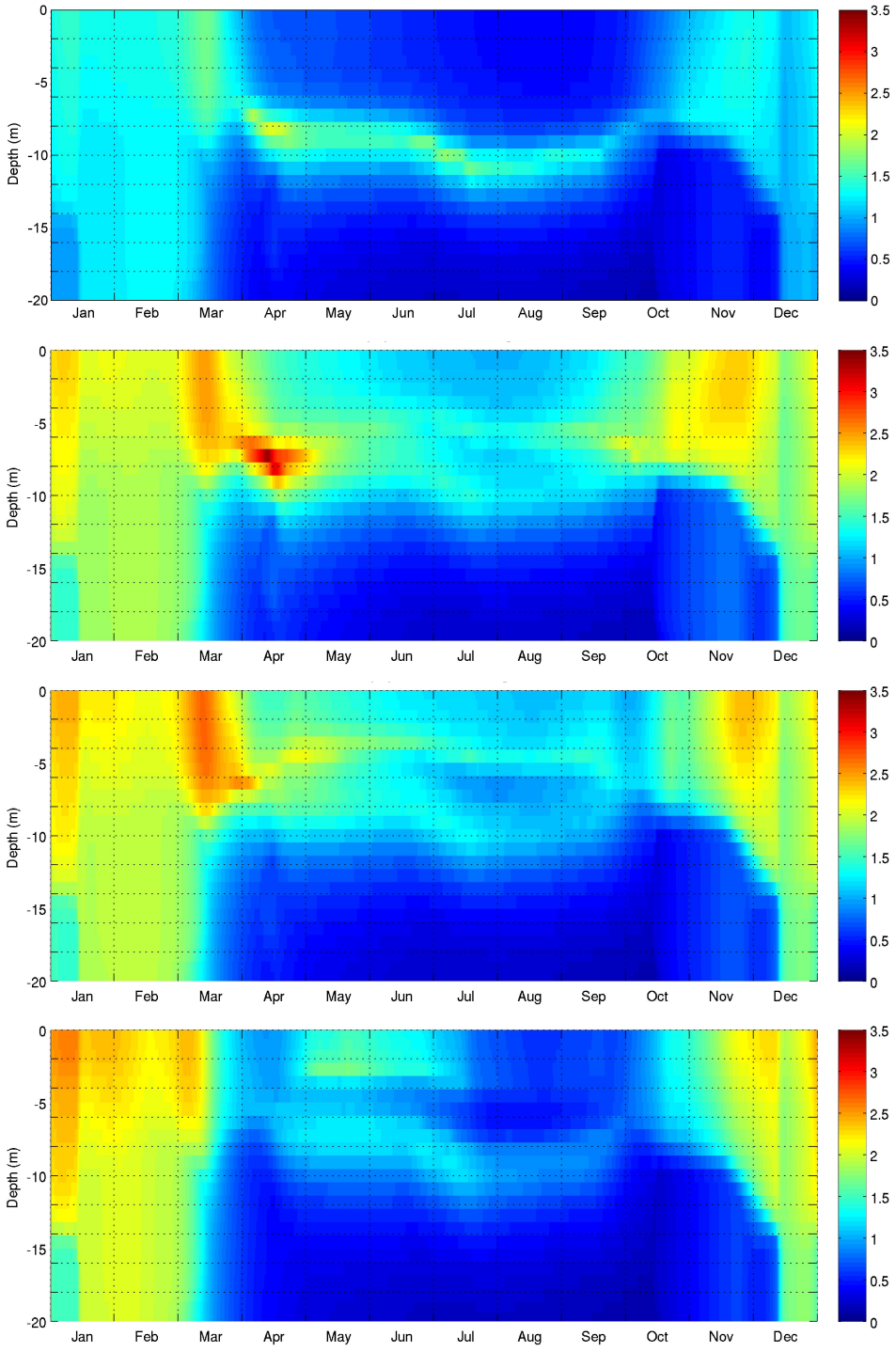

Figure 3.12: Total chlorophyll concentrations for the base experiment and runs without bacteria and closure remineralization rates of 0.05, 0.1 and 0.25 d^{-1} from top to bottom in mgC m^{-3}.

Plankton community composition

With no bacteria in the system, all phytoplankton groups (diatoms, nanoflagellates and picophytoplankton) concentrations rise. Figure 3.13 represents nanoflagellates in the base experiment and their response to the increasing remineralization rate in terms of carbon content.

The base experiment hows lowest concentrations. At a low remineralization rate (0.05 - 0.1 d^{-1}), the peak concentration of carbon in nanoflagellates occurs in April-May, revealing the spring bloom. This bloom remains shallow in the top 4m and is very compact. As nutrient availability rises, the carbon concentration of the bloom starts to increase denoting a higher number of organisms. Moreover, the bloom period stretches until June at a remineralization rate of 0.25 d^{-1} and to September at higher rates. In all cases however, the bloom never outreaches 4m depth and remains in the shallow surface area.

Even though the extent of the bloom increases, maximum carbon concentrations still occur between April and May, highlightling that this is the optimal period for blooming (spring) especially in terms of light and nutrients availability. The constant high values from April to September at high remineralization rates underline the unrealistic situation of constant high nutrient availability, which coupled to light intensity results in a continual, elongated bloom.

The choice of representing nanoflagellates was dictated by the fact that compared to the base experiment, they show the strongest change together with picophytoplankton.

The above described change in primary producers' distribution causes a consequent shift, or rather increment, in the zooplankton community. Peak zooplankton concentration occurs in concomitance to the peak carbon concentration in phytoplankton (figure 3.11). In fact, the increase in remineralization and phytoplankton biomass causes this zooplankton concentration rise. All zooplankton groups show a marked rise in concentration with microzooplankton always being the more abundant, followed by flagellates heterotrophs and mesozooplankton. Also, as remineralization increases the zooplankton peak shifts slightly along the year towards May and extending to July. During the period of high abundance, from the second half of March to half December, the bottom 10m of the water column remains low in concentration. The rest of the year shows a uniform distribution throughout the water column. The total carbon in the zooplankton Hovmöller plot is very similar to those of pico and nanoplakton, suggesting a diet poor in diatoms.

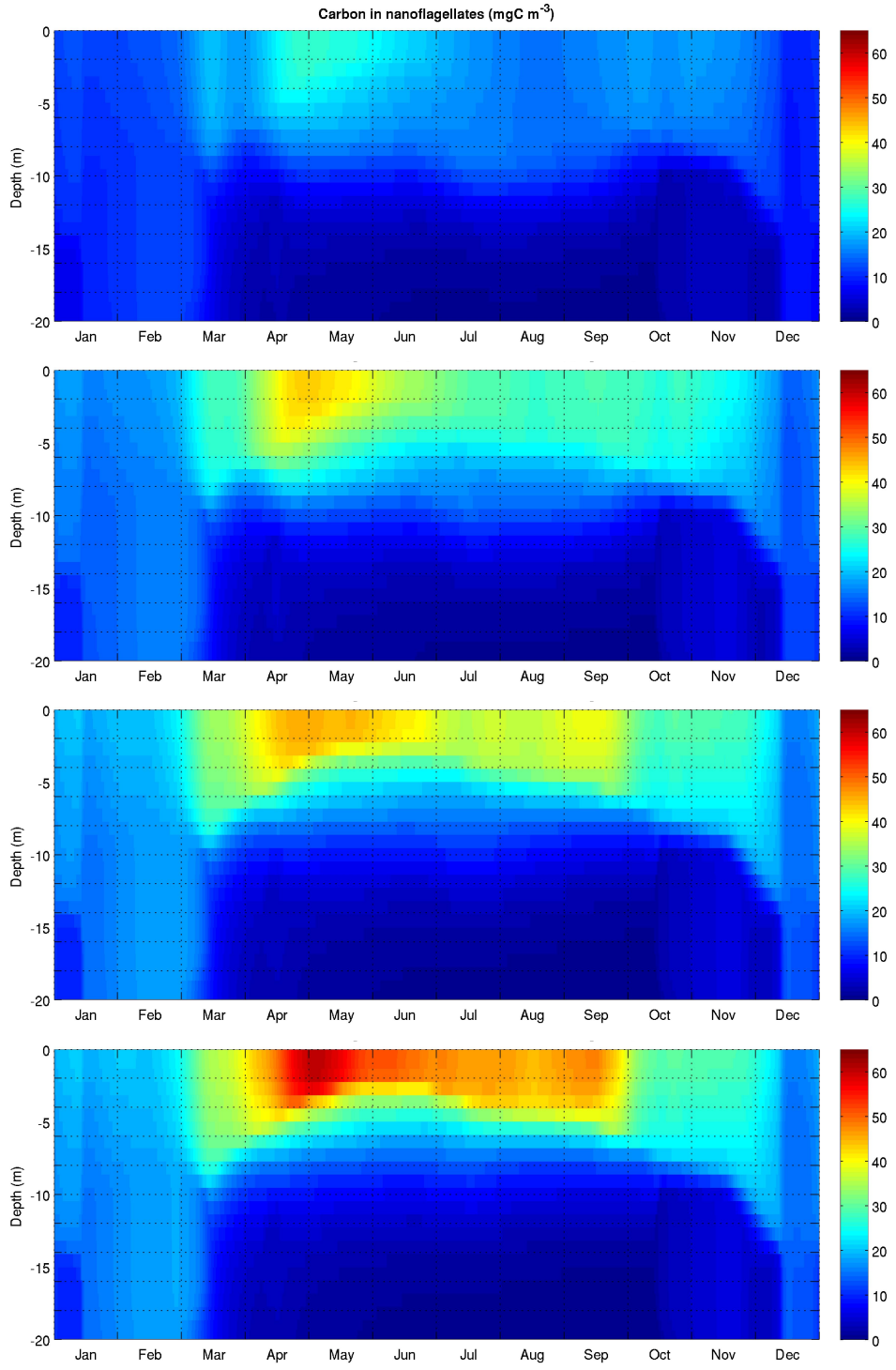

Figure 3.13: Carbon concentrations in nanoflagellates for the base experiment and experiment 1 with closure remineralization rates of 0.05, 0.25 and 0.75 d^{-1} from top to bottom in mgC m^{-3}

Nutrients

When bacteria are removed from the system, concentrations of both ammonia and nitrate decrease drastically, despite maintaining the same shape, signifying a high consumption rate, while phosphate concentration increases. It was chosen to represent only phosphate results (figure 3.14) seen the model's higher error for nitrates. When remineralization increases more nutrients are recycled in the water column and are available for consumption. In fact, phosphate increases from the closure remineralization rate of 0.05 d^{-1} to 0.25 d^{-1} . However, at higher remineralization rates phsophate concentrations stop increasing and stabilize. Highest concentrations are found on the seafloor as already seen in the base experiment, and during summer months. With increasing remineralization rates, higher concentrations reach upper in the water column creating a situation where low concentrations are only found between March and April in the top part of the water column.

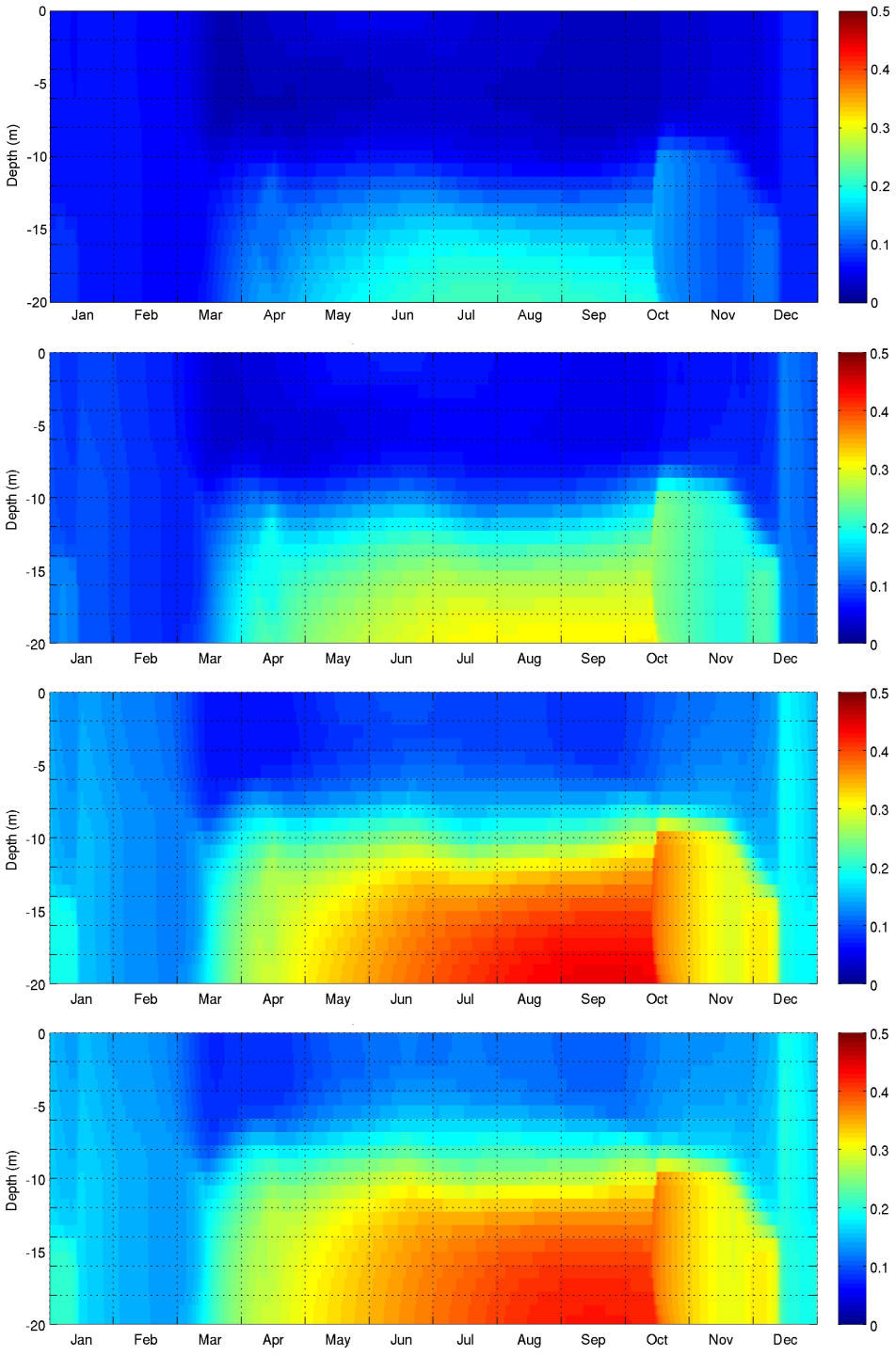

Figure 3.14: Phsophate concentration for the base experiment and experiment 1 with implicit remineralization rates of 0.05,0.25 and 0.75 d^{-1} from top to bottom in mmol m^{-3}

3.2.1 Experiment 1a - No bacteria and no closure remineralization

Rationally speaking, in nature if one were to completely remove bacteria from the system, the remineralization rate would fall to zero. The following experiment consists in setting the remineralization rate (pelagic and benthic) to zero in order to mimic such a situation and to test the model sensitivity. In a simple normal NPZD model, setting the closure remineralization to a null value would cause the model to become unstable. However, in our model this does not happen because although there is no process or organism to convert the detritus back to nutrients, the loop is closed by microzooplankton which acts as remineralizer through excretion (figure 3.15).

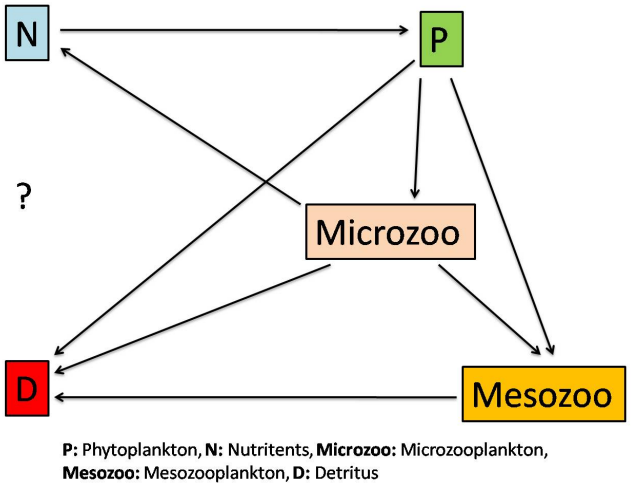

Figure 3.15: A simplified schematic of POM1D-BFM to show what happens in the system when bacteria are removed and the closure remineralization rate falls to zero

In such a condition, the total carbon detritus is most representative as most of the system ends up in this compartment. Figure 3.16 shows the total carbon detritus for the base experiment and experiment 1a. While in the base experiment concentrations are highest during summer due to the higher productivity, with no closure remineralisation taking place, there is a gradual accumulation of detritus along the year as there is nothing in the system to convert this back to usable nutrients. Here the base experiment scale has been adjusted to the experiment 1a scale, and this highlights the large change in detritus concentration which takes place. In fact, detritus accumulates with time from the surface to the bottom. The composition mainly comprises of semi-liable organic matter as in the base experiment with very little POM and some DOM which however does not greatly contribute the total detritus. In this experiment, not everything falls into the detritus compartment because as seen in figure 3.15, microzooplankton acts as nutrient remineralizer returning back to the system available

nutrients via excretion. However, this path is not enough to keep the system up and in fact, with time nearly everything dies and falls into the detritus compartment.

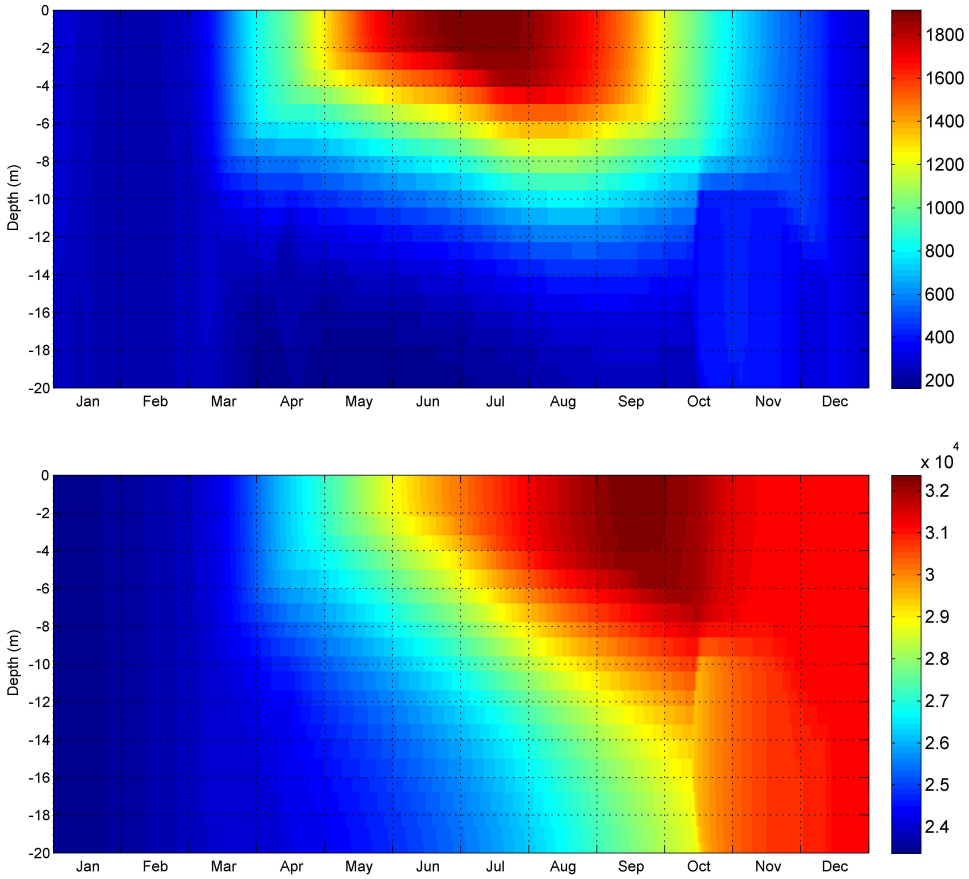

Figure 3.16: From the top, total carbon detritus in mgC m^{-3} for the base experiment and for experiment 1a (no bacteria in the system and no closure remineralization). Most of this detritus in experiment 1a is made up by dissolved organic matter (Note the difference in scale).

Regarding the phytoplankton composition, the smaller remineralization taking place results in smaller quantities. Nevertheless, picophytoplankton arises above others in quantity between March and April in the top half water column. This general decrease in concentrations of phytoplankton results in less zooplankton in the system, especially mesozooplankton which remains in very low concentrations (< 1 mgC m^{-3}). Phosphate also falls to very low concentrations, suggesting its consumption, while nitrates increase.

3.3 Experiment 2 - Eliminating all microbial components

Experiment 1a demonstrated that although the bacterial component of the model was removed and the closure remineralization rate was set to zero, microzooplankton acted as remineralizers through excretion. The second experiment therefore aimed at keeping only the herbivore chain active and in order to do so, all micro components were excluded (bacteria, microzooplankton, picophytoplankton). This removed definitely the remineralization taking place through this compartment. A schematic explaining the simplification applied to the model is presented in figure 3.17.

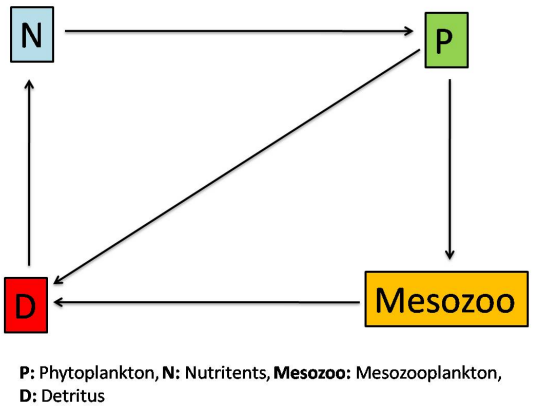

Figure 3.17: A schematic of the simplification applied to eliminate the microbial system (bacteria, picophytoplankton and microzooplankton) from the POM1D-BFM.

Figure 3.18 represents the total carbon in the detritus for the base experiment and for closure remineralization rates of 0.05, 0.25 and 0.75d^{-1}. For all trials with different rimineralization rates, DOM was null, POM was in moderate concentrations while semi-liable carbon was the major contributor to the total carbon in the detritus. As expected, the total detritus concentration decreases to very low values with increasing remineralization. The remineralization recycles detritus in the water column converting it to available nutrients and therefore, with more recycling taking place, less detritus is left. Also, the elimination of the microbial components from the system causes a large increase in the amount of total detritus. For experiments with remineralization rates of 0.75 and 1d^{-1} concentrations were very low, as for the base experiment.

Similarly to experiment 1 and 1a, phosphate concentrations decrease with increasing remineralization rates, while nitrate increases. In both cases however, concentrations are higher in respect to the same remineralization rates of experiment 1.

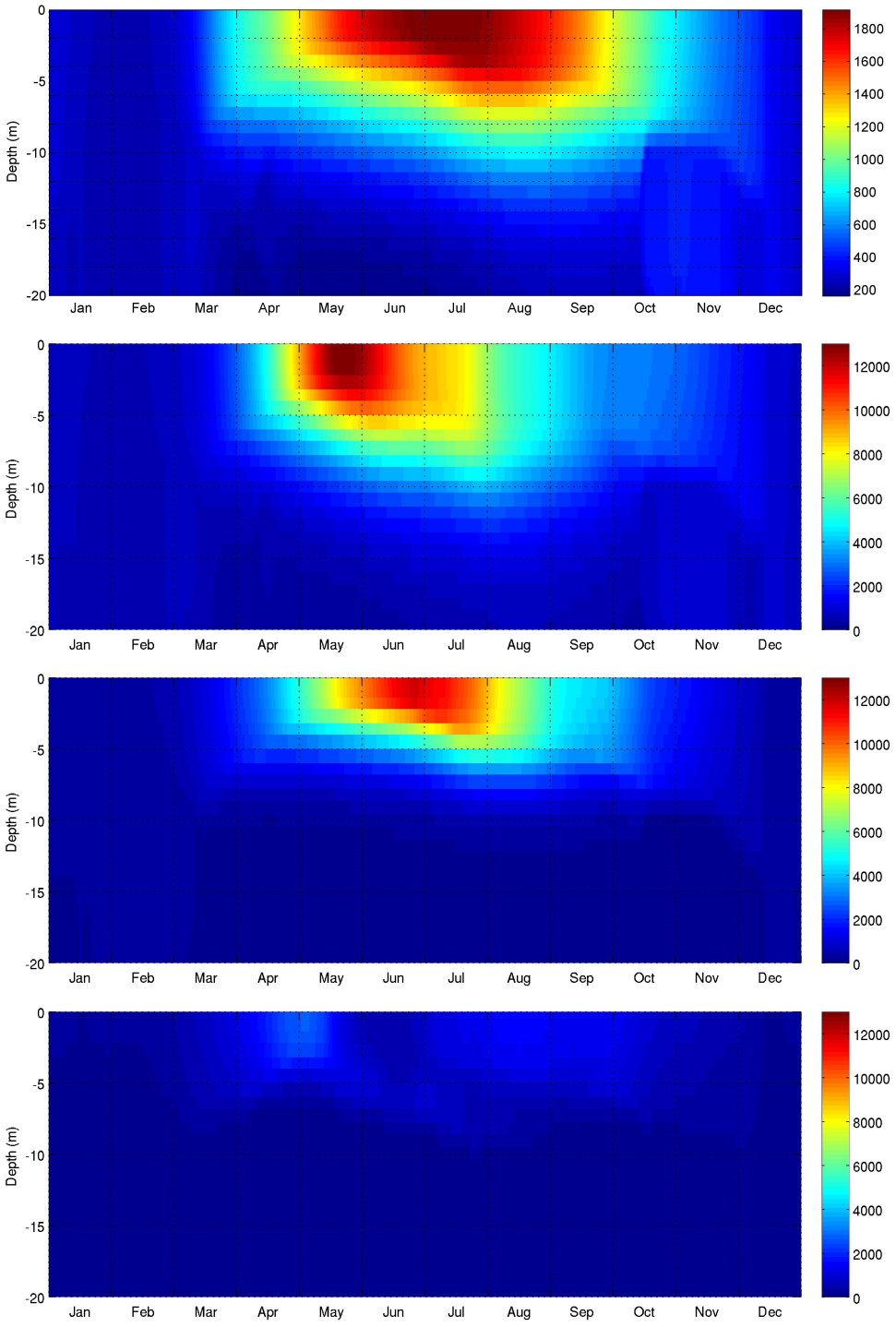

Figure 3.18: From the top, total carbon detritus concentrations in mgC m^{-3} for the base experiment and for experiment 2 (no microbial system) with closure remineralization rates of 0.05, 0.25 and 0.75 d^{-1} (Note the difference in scale for the base experiment)

Plankton composition and biomass

This experiment has only diatoms and nanoflagellates in the system. Naturally, as already seen, the concentrations of these two groups grow with increasing remineralization, however their maximum concentrations occur in a different period of the year. Also, the removal of picophytoplankton from the system results in less competition between them and therefore concentrations globally rise. For diatoms, maximum concentrations occur from May to July marking the subsurface chlorophyll maximum. The shape of the distribution does not change much from experiment 1, in contrast to nanoflagellates which see a remarkable difference. In fact, nanoflagellates concentrations stay low throughout the whole water column until June, when a large bloom takes place in the top half water column until December. This can be seen in figure 3.19 showing carbon in nanoflagellates concentrations for the base experiment and remineralization rates of 0.05,0.75 and 1 d^{-1}. Nanoflagellate biomass grows exponentially with the increasing of the remineralization rate, especially for values above $0.75d^{-1}$. Contrastingly, the diatoms biomass increases very quickly and slows down around a rimineralization value of 0.5 d^{-1} (figure 3.20). Also, their distribution during the year does not undergo large changes, rather an intensification during the summer months in the subsurface chlorophyll maximum. For both nanoflagellates and diatoms, concentrations of the base experiment are much lower, underlining the high model sensitivity.

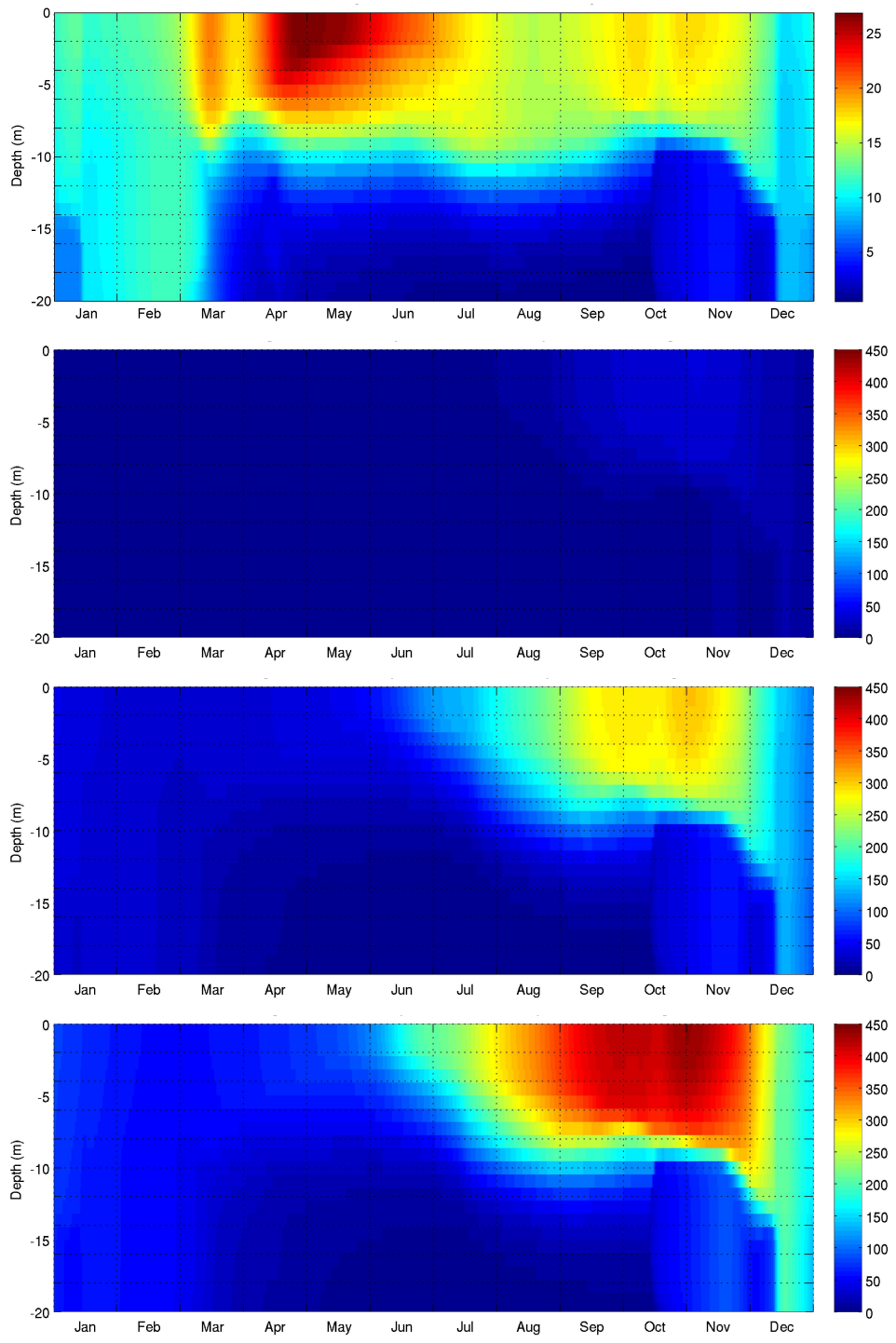

Figure 3.19: Carbon in nanoflagellates concentrations in mgC m^{-3} for the base experiment and experiment 2 (no microbial system) with the closure remineralization rates of 0.5, 0.75 and 1 d^{-1} from top to bottom (Note the difference in scale for the top two graphs.)

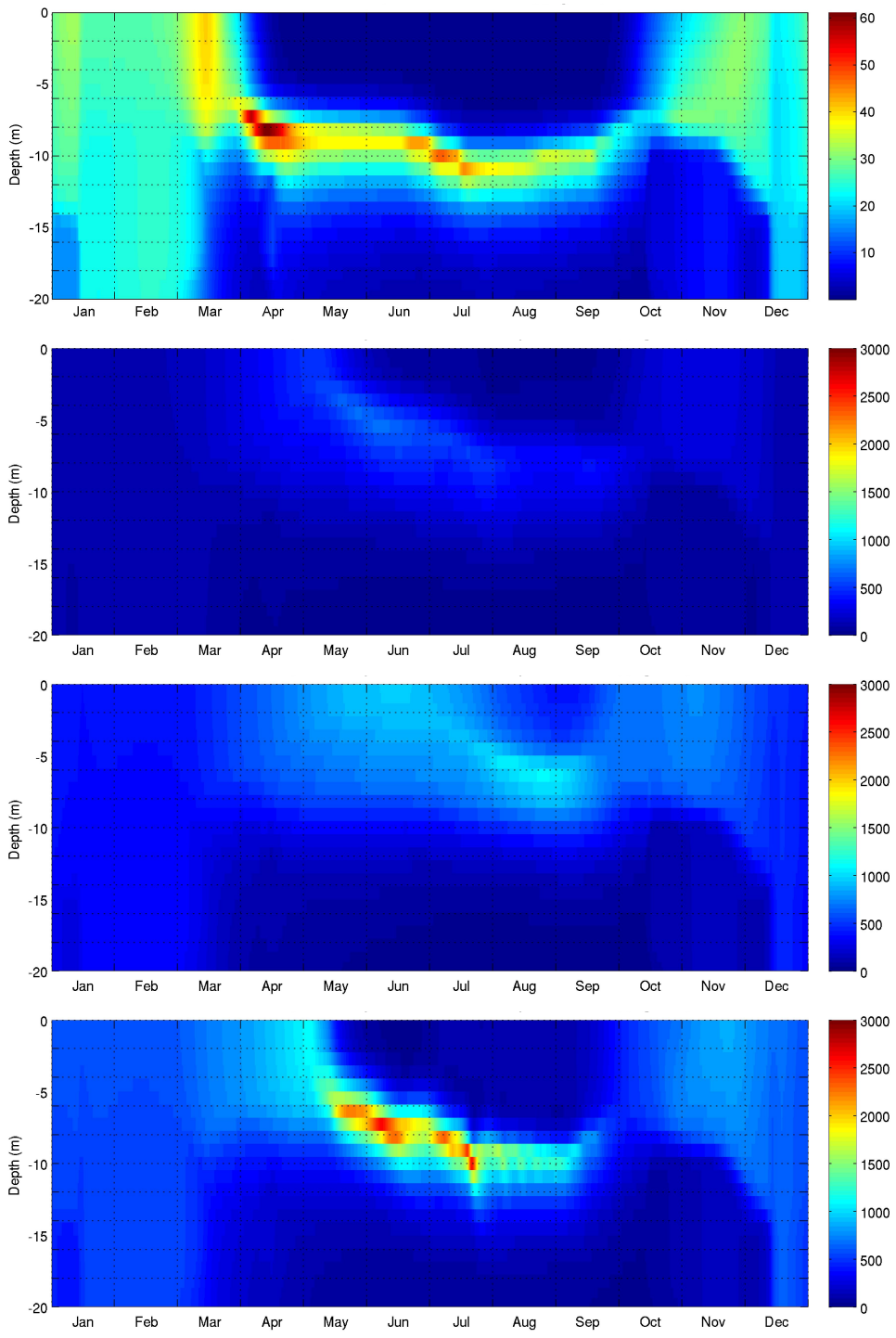

Figure 3.20: Carbon in diatoms for the base experiment and experiment 2 (no microbial system) with closure remineralization rates of 0.05, 0.25 and 0.75d^{-1} from top to bottom (Note the difference in scale for the base experiment).

Chapter 4

Discussion and conclusions

A numerical model consisting of the 1-D version of the Princeton Ocean Model (POM) coupled to the Biological Flux Model was used in a "mechanistic" way to be able to demonstrate the importance of the different functional ecosystem components in the organic carbon flux dynamics. The aim was to understand the low trophic level ecosystem structure in the Gulf of Trieste with the objective of investigating the microbial role in the carbon cycling and the competition between plankton and bacteria on nutrients cycling.

The base experiment and the comparison of model results with observations demonstrates that the model is only marginally capable of reproducing the typical chlorophyll and nutrients distributions in the water column. In the case of nitrates, the model is unable to mimic observations even qualitatively. More calibration of nutrient inputs should be done, however the mechanistic strategy can be followed only considering it will not be so relevant for the realistic case.

The base experiment shows a phosphate peak near the seabed from June to September and this could be linked to the phosphate rich particulate organic matter which sinks to the seafloor and is then remineralized by bacteria in the benthic compartment. The low concentrations on the surface during the year emphasise how river influence is not considered propely in the model.

The base experiment showed how picophytoplankton, nanoflagellates and bacteria all bloom during the same period and in the same area where diatom concentration is low. This behaviour might be associated to a lower light sensitivity compared to diatoms and to a lower nutrient requirement as the nutrient profiles suggest. In fact, certain surrounding conditions could be favourable to a phytoplankton group but not to another.

The removal of bacteria from the system in experiment 1 has two major consequences related to their role: the reduction of remineralization in the system (which is

however compensated by the forced closure remineralization) and the removal of competition with phytoplankton for nutrients. This reduction in competition can be seen by increase of the overall planktonic biomass as a consequence of more nutrients being available for all groups. Moreover, the elimination of bacteria causes an expected increment in phosphate concentration, but an unexpected decrease in nitrate and ammonia concentrations. As Jansson (1988) argues, bacteria have higher affinity for phosphate than phytoplankton meaning that the phosphorus limitation is normally driven by the competition between bacteria and phytoplankton. Once bacteria are removed, phosphate is "left over" while nitrates and ammonia are efficently uptaken by the plankton community and are subject to a reduction in concentration. This inversion suggests a change in the limiting nutrient from phosphate to nitrate. This also renforces the theory of bacterial competition with phytoplankton for nutrients, especially for phosphorus. Moreover, the fact that in the base experiment the system is at equilibrium supports Azam and Ammerman (1984) who argued that phytoplankton production is regulated by feedback interactions, which optimize the use of dissolved inorganic nutrients at low concentrations. In fact, the competition between phytoplankton and bacteria reduces the available phosphate for phytoplankton and therefore limits its growth, but at the same time stimulates the remineralization role of bacteria.

These results indicate that the common definition of the northern Adriatic being phosphorus limited is dictated by the presence of bacteria. Moreover, these experiments support Cushing (1989) theory that the microbial web predominates in stratified waters. As a matter of fact, if the herbivore food web were to predominate, the limiting nutrient would be nitrate rather than phosphate as partly seen in experiment 1.

Furthermore, the removal of bacteria causes a shift in the plankton community composition mostly favoring picophytoplankton and nanoflagellates, rather than diatoms. This is associated to the lower competition for nutrients and has important implications on how the bacterial population shapes the ambient trophic chain and the importance of nutrient competition. In fact, no competition for nutrients at microbial levels has implications on larger scales as it favors the development of the herbivore trophic chain and therefore of bigger organisms. Less competition, more nutrients available and the development of larger organisms (zooplankton) result in an equilibrium state which shifts from a "bottom-up" control situation (growth controlled by nutrients availability) to a "top-down" one (growth controlled by predatos (zooplankton)). In fact, the different remineralization rates indicate that the nutrient pool is completely at phytoplankton's disposal not having to compete with bacteria. Additionally, in experiment 1 the abundance of flagellates heterotrophs diminuishes compared to the base experiment and this is a consequence of the fact that their diet is includes bacteria.

In experiment 1a however, when the implicit closure remineralization is removed from the system, phosphate decreases while nitrate increases. This could have a double meaning: either microzooplankton have a stronger role in the remineralization of nitrate than in that of phosphate, or more phosphate is required by the system relative to nitrate. Nonetheless, seen the results of experiment 1, the first hypothesis is more likely to be correct.

Regarding experiment 2, the increase in the amount of total detritus is due to the smaller amount of nutrient remineraliztion taking place as a consequence of the removal of microzooplankton which also act as remineralizers. Also, the vast quantity of semi-liable detritus is a consequence of the very small concentration or even absence of available nutrients because of low remineralization. The gross primary production (GPP), which is limited by temperature and light, and not by nutrients, uptakes carbon that is consequently expelled as semi-liable detritus in a condition of low nutrient availability. In fact, the more oligotrophic the system is, the greater amount of semi-liable detritus will be in the system. In a condition with high nutrients availability, bacteria would utilize this semi-liable detritus. Moreover, remineralization demolishes the semi-liable detritus and this can be seen in experiment 2. The higher the remineralization rate, the lower the semi-liable detritus in they system.

Overall, the experiments carried out suggested that remineralization closure parameters over 0.5 d^{-1} are unrealistic. The results emphasize the model's high sensitivity to small changes in the system, and with more calibration done, its reliability on representing responses to unrealistic situations. The limitations of this study include the weak nutrient inputs calibration and the scarse observational dataset, especially regarding nutrients.

In conclusion we argue that the reduction of the system to a chain without bacteria, picophytoplankton and microzooplankton produces a system shift from P-limited to N-limited and a system shift from "bottom-up" to "top-down" control.

Furthermore, we have shown that bacteria competes with phytoplankton, limiting to a certain extent its growth playing a key role in such estuarine systems. More work is needed to thoroughly understand the carbon cycle in coastal ecosystems. In particular the basic model should be better calibrated and the closure parametrizations should be further investigated. Also, more work should be done to calibrate and understand the benthic dynamics.

Acknowledgments

I would like to thank my advisor Prof. Nadia Pinardi who dedicated time to my learning, guided me and shared her broad knowledge in oceanography. Also, thank you to Marco Zavatarelli who taught and introduced me to the world of Fortran codes and numerical modelling. Without them both this thesis wouldn't have been possible.

Thank you to Alessandra Giorgetti and the biological department of Trieste, and to Cosimo Solidoro who was responsible for the projects during which most of the recent data was collected (Mitili, Ecomadr).

A huge thank you to Dott. Luca Giacomelli who supported me at SiNCEM laboratory from a computing point of view as well as from a human side. His humor and long talks made days shorter. Also, thank you very much to Claudia Fratianni and Simona Simoncelli from INGV for sharing thoughts, knowledge and happy moments.

Finally, an infinite thank you to mum, dad, Matteo, Irene and Antonio who always supported me in all my choices and trips, and were always there to take care of me during difficult moments. None of this would have been possible without their constant encouragement and love.

Bibliography

Allen, A., Howard-Jones, M., Booth, M., Frischer, M., Verity, P., Bronk, D., Sanderson, M., 2002. Importance of heterotrophic bacterial assimilation of ammonium and nitrate in the barents sea during summer. Journal of Marine Systems 38 (1-2), 93–108.

Aota, Y., Nakajima, H., 2000. Mathematical analysis on coexistence conditions of phytoplankton and bacteria systems with nutrient recycling. Ecological Modelling 135 (1), 17 – 31.

Artegiani, A., Bregant, D., Paschini, E., Pinardi, N., Raicich, F., Russo, A., 1997a. The adriatic sea general circulation .1. Air-sea interactions and water mass structure. Journal of Physical Oceanography 27 (8), 1492–1514.

Artegiani, A., Bregant, D., Paschini, E., Pinardi, N., Raicich, F., Russo, A., AUG 1997b. The Adriatic Sea general circulation .2. Baroclinic circulation structure. Journal of Physical Oceanography 27 (8), 1515–1532.

Azam, F., 1998. Microbial control of oceanic carbon flux: The plot thickens. Science 280 (5364), 694–696.

Azam, F., 2000. New approaches to integrating the mcrobial loop in the functioning of the mediterranean ecosystem. In: Berman, T., Briand, F. (Eds.), Investigating marine microbial loops: new tools and perspectives. CIESM, pp. 19–20.

Azam, F., Ammerman, J. W., 1984. Cycling of organic matter by bacterioplankton in pelagic marine ecosystems: microenvironmental considerations. In: Fasham, M. J. R. (Ed.), Flow of energy and materials in marine ecosystems. Plenum, pp. 345–360.

Azam, F., Fenchel, T., Field, J. G., Gray, J. S., Meyer-Reil, L. A., Thingstad, F., 1983. The ecological role of water-column microbes in the sea. Marine Ecology Progress Series. 10, 257–263.

Azam, F., Fry, J., Williams, P., Herndl, G., 2000. Investigating marine microbial loops: new tools and perspectives. Vol. 11 of CIESM Workshop Series. CIESM.

Baines, S. B., Pace, M. L., 1991. The production of dissolved organic matter by phytoplankton and its importance to bacteria: Patterns across marine and freshwater systems. Limnology and Oceanography 36 (6), pp. 1078–1090.

Baretta, J., Ebenhoh, W., Ruardij, P., 1995. The european regional seas ecosystem model, a complex marine ecosystem model. Netherlands Journal of Sea Research 33 (3-4), 233 – 246.

Bianchi, D., Zacatarelli, M., Pinardi, N., Capozzi, R., Capotondi, L., Corselli, C., Masina, S., 2006. Simulations of ecosystem response during sapropel s1 depositti on event. Palaeogeography Palaeoclimatology Palaeoecology 235.

Bidle, K., Azam, F., Feb. 1999. Accelerated dissolution of diatom silica by marine bacterial assemblages. letters to Nature 397, 508–512.

Blackford, J., Allen, J., Gilbert, F., 2004. Ecosystem dynamics at six contrasting sites: a generic modelling study. Journal of Marine Systems 52 (1-4), 191–215.

Blumberg, A., Mellor, G., 1983. Diagnostic and prognostic numerical circulation studies of the South Atlantic Bight. Journal of Geophysical Research 88, 4579–4592.

Boehme, S. E., Sabine, C. L., Reimers, C. E., 1998. Co2 fluxes from a coastal transect: a time-series approach. Marine Chemistry 63 (1-2), 49 – 67.

Bogunovic, B., Malacic, V., March 2009. Circulation in the Gulf of Trieste: Measurements and model results. Il Nuovo Cimento C, 301–326.

Bolin, B., Degens, E. T., Kempe, S., Ketner, P., 1979. The Global Carbon Cycle. SCOPE 13. Scientific Committee on Problems of the Environment, International Council of Scientific Unions.

Butenschon, M., Zavatarelli, M., Vichi, M., 2012. Sensitivity of a marine coupled physical biogeochemical model to time resolution, integration scheme and time splitting method. Ocean Modelling 52-53 (0), 36 – 53.

Cantoni, C., Cozzi, S., Pecchiar, I., Cabrini, M., Mozetic, P., Catalano, G., Umani, S. F., 2003. Short-term variability of primary production and inorganic nitrogen uptake related to the environmental conditions in a shallow coastal area (gulf of trieste, n adriatic sea). Oceanologica Acta 26 (5-6), 565 – 575.

Cardin, V., Bensi, M., Pacciaroni, M., 2011. Variability of water mass properties in the last two decades in the South Adriatic Sea with emphasis on the period 2006-2009. Continental Shelf Research 31 (9), 951–965.

Caron, D. A., Goldman, J. C., Dennett, M. R., 1988. Experimental demonstration of the roles of bacteria and bacterivorous protozoa in plankton nutrient cycles. hydrobiologia 159 (1), 27–40.

Celio, M., Malacic, V., Bussani, A., Cermelj, B., Comici, C., Petelin, B., 2006. The coastal scale observing system component of adricosm: Gulf of trieste network. Institute of Oceanography and Fisheries, Split.

Cho, B., Azam, F., May 1990. Biogeochemical significance of bacterial biomass in the ocean's euphotic zone. Marine Ecology - Progress Series 63 (2-3), 253–259.

Conversi, A., Peluso, T., Fonda-Umani, S., 2009. Gulf of Trieste: A changing ecosystem. Journal of Geophysical Research - Oceans 114.

Crisciani, F., 1995. Osservazioni meteomarine eseguite a Trieste nel trentennio 1965-1994. C.N.R.-Istituto sperimentale talassografico.

Cushing, D., 1989. A difference in structure between ecosystems in strongly stratified waters and in those that are only weakly stratified. Journal of Plankton Research 11 (1), 1–13.

Cushman-Roisin, B., Gačić, M., Poulain, P., 2001. Physical oceanography of the Adriatic Sea: past, present, and future. Kluwer Academic Publishers.

Danger, M., Leflaive, J., Oumarou, C., Ten-Hage, L., Lacroix, G., 2007a. Control of phytoplankton-bacteria interactions by stoichiometric constraints. Oikos 116 (7), 1079–1086.

Danger, M., Oumarou, C., Benest, D., Lacroix, G., 2007b. Bacteria can control stoichiometry and nutrient limitation of phytoplankton. Functional Ecology 21 (2), 202–210.

De Senerpont Domis, L., Mooij, W., Huisman, J., 2007. Climate-induced shifts in an experimental phytoplankton community: a mechanistic approach. Hydrobiologia 584, 403–413.

De Vittor, C., Paoli, A., Fonda Umani, S., 2008. Dissolved organic carbon variability in a shallow coastal marine system (Gulf of Trieste, northern Adriatic Sea). Estuarine, Coastal and Shelf Science 78 (2), 280–290.

Dickey, T., Plueddemann, A. J., Weller, R., 1998. Current and water property measurements in the coastal ocean. In: Robinson, A. R., Brink, K. (Eds.), The Sea. Vol. 10. Harvard University Press, Cambridge, USA, Ch. 14, pp. 367 – 398.

Ducklow, H. W., Steinberg, D. K., Buesseler, K. O., 2001. Upper ocean carbon export and the biological pump. The Oceanography Society 14 (4), 50–58.

Ducklow, W. H., McCallister, S. L., 2004. The biogeochemistry of carbon dioxide in the coastal oceans. In: The global coastal ocean - Multiscale interdisciplinary processes. Harvard University Press, Ch. 9, pp. 269–315.

Dufour, P., Torreton, J.-P., 1996. Bottom-up and top-down control of bacterioplankton from eutrophic to oligotrophic sites in the tropical northeastern atlantic ocean. Deep Sea Research Part I: Oceanographic Research Papers 43 (8), 1305 – 1320.

Fennel, K., Losch, M., Schroter, J., Wenzel, M., 2001. Testing a marine ecosystem model: sensitivity analysis and parameter optimization. Journal of Marine Systems 28 (1-2), 45 – 63.

Fonda Umani, S., 2005. Relationships between microzooplankton and mesozooplankton: competition versus predation on natural assemblages of the gulf of trieste (northern adriatic sea). Journal of Plankton Research 27 (10), 973–986.

Fonda Umani, S., Del Negro, P., Larato, C., De Vittor, C., Cabrini, M., Celio, M., Falconi, C., Tamberlich, F., Azam, F., 2007. Major inter-annual variations in microbial dynamics in the gulf of trieste (northern adriatic sea) and their ecosystem implications. Aquatic Microbial Ecology 46 (2), 163–175.

Friedrichs, M. A. M., Dusenberry, J. A., Anderson, L. A., Armstrong, R. A., Chai, F., Christian, J. R., Doney, S. C., Dunne, J., Fujii, M., Hood, R., McGillicuddy, Jr., D. J., Moore, J. K., Schartau, M., Spitz, Y. H., Wiggert, J. D., AUG 2 2007. Assessment of skill and portability in regional marine biogeochemical models: Role of multiple planktonic groups. Journal of Geophysical Research - Oceans 112 (C8).

Gacic, M., Marullo, S., Santoleri, R., Bergamasco, A., 1997. Analysis of the seasonal and interannual variability of the sea surface temperature field in the Adriatic Sea from AVHRR data (1984-1992). Journal of Geophysical Research - Oceans 102 (C10), 22937–22946.

Gibson, J., Kallberg, P., Uppala, S., Nomura, A., Serrano, E., 1997. ERA description, ECMWF re-analysis project report series 1. No. v. 1. ECMWF.

Giovannoni, S. J., Stingl, U., 2005. Molecular diversity and ecology of microbial plankton. Nature 437 (7057), 343–348.

Goldman, J. C., Caron, D. A., Dennett, M. R., 1987. Regulation of gross growth efficiency and ammonium regeneration in bacteria by substrate c:n ratio. Limnology and Oceanography 32 (6), pp. 1239–1252.

Jansson, M., 1988. Phosphate uptake and utilization by bacteria and algae. Hydrobiologia 170, 177–189.

Jiao, N., Azam, F., 2011. Microbial carbon pump and its significance for carbon sequestration in the ocean. In: Microbial carbon pump in the ocean. Science/AAAS, Ch. 2, pp. 43–45.

Jiao, N., Azam, F., Sanders, S., 2011. Microbial carbon pump in the ocean. Science/AAAS.

Jiao, N., Herndl, G. J., Hansell, D. A., Benner, R., Kattner, G., Wilhelm, S. W., Kirchman, D. L., Weinbauer, M. G., Luo, T., Chen, F., Azam, F., Aug. 2010. Microbial production of recalcitrant dissolved organic matter: long-term carbon storage in the global ocean. Nature reviews. Microbiology 8 (8), 593–599.

Jiao, N., Zheng, Q., 2011. The microbial carbon pump: From genes to ecosystems. Applied and Environmental Microbiology 77 (21), 7439–7444.

Jumars, P. A., Penry, D. L., Baross, J. A., Perry, M. J., Frost, B. W., 1989. Closing the microbial loop: dissolved carbon pathway to heterotrophic bacteria from incomplete ingestion, digestion and absorption in animals. Deep Sea Research Part A. Oceanographic Research Papers 36 (4), 483 – 495.

Kirchman, D. L., 1994. The uptake of inorganic nutrients by heterotrophic bacteria. Microbial Ecology 28, 255–271.

Kriest, I., Khatiwala, S., Oschlies, A., 2010. Towards an assessment of simple global marine biogeochemical models of different complexity. Progress In Oceanography 86 (3-4), 337 – 360.

Legendre, L., Rassoulzadegan, F., 1995. Plankton and nutrient dynamics in marine waters. Ophelia 41 (1), 153–172.

Lima, I., Olson, D., Doney, S., 2002. Intrinsic dynamics and stability properties of size-structured pelagic ecosystem models. Journal of Plankton Research 24 (6), 533–556.

Lipizer, M., Vittor, C. D., Falconi, C., Comici, C., Tamberlich, F., Giani, M., 2012. Effects of intense physical and biological forcing factors on cnp pools in coastal waters (gulf of trieste, northern adriatic sea). Estuarine, Coastal and Shelf Science.

Mackenzie, F. T., Andersson, A., Lerman, A., May Ver, L., 2004. Boundary exchanges in the global coastal margin: implications for the organic and inorganic carbon cycles. In: The global coastal ocean - Multiscale interdisciplinary processes. Harvard University Press, Ch. 7, pp. 193–225.

Maggiore, A., Zavatarelli, M., Angelucci, M., Pinardi, N., 1998. Surface heat and water fluxes in the adriatic sea: Seasonal and internanual variability. Physics and Chemistry of The Earth 23 (5-6), 561 – 567.

Malacic, V., Celio, M., Cermelj, B., Bussani, A., Comici, C., 2006. Interannual evolution of seasonal thermohaline properties in the Gulf of Trieste (northern Adriatic) 1991-2003. Journal of Geophysical Research - Oceans 111 (C8).

Malacic, V., Petelin, B., 2009. Climatic circulation in the Gulf of Trieste (northern Adriatic). Journal of Geophysical Research - Oceans 114.

Malacic, V., Viezzoli, D., 1998. Tidal dynamics in the gulf of trieste - northern adriatic. Rapport de la Commission Internationale pour l'Exploration Scientifique de la Mer Mediterranee.

Malacic, V., Viezzoli, D., Jul. 2000. Tides in the northern Adriatic Sea - the Gulf of Trieste. Nuovo Cimento C Geophysics Space Physics C 23, 365.

Mauri, E., Poulain, P.-M., Notarstefano, G., 2008. Spatial and temporal variability of the sea surface temperature in the Gulf of Trieste between January 2000 and December 2006. Journal of Geophysical Research - Oceans 113 (C10).

Mellor, G., 2004. Users guide for a three-dimensional, primitive equation, numerical ocean model.

Mellor, G. L., Yamada, T., 1982. Development of a turbulence closure model for geophysical fluid problems. Rev. Geophys. Space Phys. 20 (C2), 851–875.

Mopper, K., Degens, E., 1979. Organic carbon in the ocean: Nature and cycling. In: Bolin, B., Degens, E. T., Kempe, S., Ketner, P. (Eds.), The Global Carbon Cycle. SCOPE, Ch. 11.

Mozetic, P., Umani, S., Cataletto, B., Malej, A., 1998. Seasonal and inter-annual plankton variability in the Gulf of Trieste (northern Adriatic). Ices Journal of Marine Science 55 (4), 711–722.

Nagata, T., Tamburini, C., Aristegui, J., Baltar, F., Bochdansky, A. B., Fonda-Umani, S., Fukuda, H., Gogou, A., Hansell, D. A., Hansman, R. L., Herndl, G. J., Panagiotopoulos, C., Reinthaler, T., Sohrin, R., Verdugo, P., Yamada, N., Yamashita, Y., Yokokawa, T., Bartlett, D. H., 2010. Emerging concepts on microbial processes in the bathypelagic ocean - ecology, biogeochemistry, and genomics. Deep-Sea Research Part II - Topical Studies in Oceanography 57 (16), 1519–1536.

Ogawa, H., Amagai, Y., Koike, I., Kaiser, K., Benner, R., 2001. Production of refractory dissolved organic matter by bacteria. Science 292 (5518), 917–920.

Ogrinc, N., Faganeli, J., 2006. Phosphorus regeneration and burial in near-shore marine sediments (the Gulf of Trieste, northern Adriatic Sea). Estuarine, Coastal and Shelf Science 67 (4), 579–588.

Ogrinc, N., Faganeli, J., Pezdic, J., 2003. Determination of organic carbon remineralization in near-shore marine sediments (Gulf of Trieste, Northern Adriatic) using stable carbon isotopes. Organic Geochemistry 34 (5), 681–692.

Ovchinnikov, I., Zats, V., Krivosheia, V., Udodov, A., 1985. A forming of depp eastern Mediterranean waters in the Adriatic Sea. Okeanologiya 25 (6), 911–917.

Pernthaler, J., 2005. Predation on prokaryotes in the water column and its ecological implications. Nature Reviews Microbiology 3 (9).

PICO, 2012. Requirements for global implementation of the strategic plan for coastal goos.

Pinardi, N., Zavatarelli, M., Arneri, E., Crise, A., Ravaioli, M., 2005. The physical, sedimentary and ecological structure and variability of shelf areas in the mediterranean sea. In: Robinson, A. R., Brink, K. (Eds.), The Sea. Vol. 14B. Harvard University Press, Cambridge, USA, Ch. 32, pp. 1243 – 1330.

Pirazzoli, P., Tomasin, A., 1999. Recent abatement of easterly winds in the northern Adriatic. International Journal of Climatology 19 (11), 1205–1219.

Platt, T., Geider, R., Sciandra, A., Copin-Montegut, C., Bouman, H. A., Sathyendranath, S., 2004. Dynamics and interactions of autotrophs, lights, nutrients and carbon dioxide. In: The global coastal ocean - Multiscale interdisciplinary processes. Harvard University Press, Ch. 12, pp. 375–412.

Polimene, L., Pinardi, N., Zavatarelli, M., Allen, J. I., Giani, M., Vichi, M., 2007. A numerical simulation study of dissolved organic carbon accumulation in the northern Adriatic Sea. Journal of Geophysical Research - Oceans 112 (C3).

Polimene, L., Pinardi, N., Zavatarelli, M., Colella, S., 2006a. The Adriatic Sea ecosystem seasonal cycle: Validation of a three-dimensional numerical model. Journal of Geophysical Research - Oceans 112 (C3).

Polimene, L., Pinardi, N., Zavatarelli, M., Colella, S., 2006b. The Adriatic Sea ecosystem seasonal cycle: Validation of a three-dimensional numerical model. Journal of Geophysical Research - Oceans 112 (C3).

Powell, T. M., Lewis, C. V. W., Curchitser, E. N., Haidvogel, D. B., Hermann, A. J., Dobbins, E. L., 2006. Results from a three-dimensional, nested biological-physical model of the California Current System and comparisons with statistics from satellite imagery. Journal of Geophysical Research - Oceans J 111 (C7).

Raicich, F., 1994. Note on the flow rates of the adriatic rivers. Note on the Flow Rates of the Adriatic Rivers, 8Cited By (since 1996) 52.

Robinson, A. R., Brink, K., 2004. The global coastal ocean - Multiscale interdisciplinary processes. The Sea. Harvard University Press, Cambridge, USA.

Robinson, A. R., Brink, K., 2005. The global coastal ocean. The Sea. Harvard University Press, Cambridge, USA.

Russo, A., Artegiani, A., 1996. Adriatic Sea hydrography. Scientia Marina 60 (2), 33–43, Seminar on Anchovy and Its Environment, Girona, Spain, May 30 - Jun 02, 1995.

Schartau, M., Oschlies, A., Willebrand, J., 2001. Parameter estimates of a zero-dimensional ecosystem model applying the adjoint method. Deep Sea Research Part II: Topical Studies in Oceanography 48 (8), 1769–1800.

Socal, G., Acri, F., Bastianini, M., Bernardi Aubry, F., Bianchi, F., Cassin, D., Coppola, J., De Lazzari, A., Bandelj, V., Cossarini, G., Solidoro, C., 2008. Hydrological and biogeochemical features of the northern adriatic sea in the period 2003-2006. Marine Ecology 29 (4), 449 – 468.

Solidoro, C., Bandelj, V., Barbieri, P., Cossarini, G., Fonda Umani, S., Jul. 2007. Understanding dynamic of biogeochemical properties in the northern Adriatic Sea by using self-organizing maps and k-means clustering. Journal of Geophysical Research (Oceans) 112, 7.

Solidoro, C., Bastianini, M., Bandelj, V., Codermatz, R., Cossarini, G., Melaku Canu, D., Ravagnan, E., Salon, S., Trevisani, S., Jul. 2009. Current state, scales of variability, and trends of biogeochemical properties in the northern Adriatic Sea. Journal of Geophysical Research (Oceans) 114, 7.

Spitz, Y., Newberger, P., Allen, J., Mar. 2003. Ecosystem response to upwelling off the Oregon coast: Behavior of three nitrogen-based models. Journal of Geophysical Research (Oceans) 108, 3062.

Stoderegger, K., Herndl, G. J., 1998. Production and release of bacterial capsular material and its subsequent utilization by marine bacterioplankton. Limnology and Oceanography 43 (5), pp. 877–884.

Supic, N., Orlic, M., 1999. Seasonal and interannual variability of the northern Adriatic surface fluxes. Journal of Marine Systems 20 (1-4), 205–229.

Tedesco, L., Vichi, M., 2010. BFM-SI: A new implementation of the Biogeochemical Flux Model in sea ice.

Thingstad, T. F., Rassoulzadegan, F., 1995. Nutrient limitations, microbial food webs, and biological C-pumps: suggested interactions in a P-limited Mediterranean. Marine Ecology - Progress Series 117 (1-3), 299–306.

Tian, R., Vezina, A., Legendre, L., Ingram, R., Klein, B., Packard, T., Roy, S., Savenkoff, C., Silverberg, N., Therriault, J., Tremblay, J., 2000. Effects of pelagic food-web interactions and nutrient remineralization on the biogeochemical cycling of carbon: a modeling approach. Deep Sea Research Part II: Topical Studies in Oceanography 47 (3-4), 637 – 662.

Totti, C., Civitarese, G., Acri, F., Barletta, D., Candelari, G., Paschini, E., Solazzi, A., 2000. Seasonal variability of phytoplankton populations in the middle Adriatic sub-basin. Journal of Plankton Research 22 (9), 1735–1756.

Vasseur, D. a., McCann, K. s., 2005. A mechanistic approach for modeling temperature-dependent consumer-resource dynamics. The American Naturalist 166 (2), 184–198.

Vichi, M., Masina, S., Navarra, A., 2007. A generalized model of pelagic biogeochemistry for the global ocean ecosystem. Part II: Numerical simulations. Journal of Marine Systems 64 (1-4), 110–134.

Vichi, M., Masina, S., Navarra, A., 2007. A generalized model of pelagic biogeochemistry for the global ocean ecosystem. part ii: Numerical simulations. Journal of Marine Systems 64 (1-4), 110 – 134.

Vichi, M., Oddo, P., Zavatarelli, M., Coluccelli, A., Coppini, G., Celio, M., Umani, S., Pinardi, N., 2003. Calibration and validation of a one-dimensional complex marine biogeochemical flux model in different areas of the northern Adriatic shelf. Annales Geophysicae 21 (1, Part 2), 413–436.

Vichi, M., Pinardi, N., Masina, S., 2007. A generalized model of pelagic biogeochemistry.for the global ocean ecosystem. Part I: Theory. Journal of Marine Systems 64 (1-4), 89–109, Symposium on Advances in Marine Ecosystem Modelling Research, Plymouth, England, Jun 27-29, 2005.

Vichi, M., Pinardi, N., Zavatarelli, M., Matteucci, G., Marcaccio, M., Bergamini, M., Frascari, F., 1998a. One-dimensional ecosystem model tests in the po prodelta area (northern adriatic sea). Environmental Modelling and Software 13, 471–481.

Vichi, M., Zavatarelli, M., Pinardi, N., 1998b. Seasonal modulation of microbially mediated carbon fluxes in the northern adriatic sea. Fisheries Oceanography 7 (3-4), 182–190.

Vilibic, I., 2003. An analysis of dense water production on the North Adriatic shelf. Estuarine, Coastal and Shelf Science 56 (3-4), 697–707.

Vilibic, I., Grbec, B., Supic, N., 2004. Dense water generation in the north Adriatic in 1999 and its recirculation along the Jabuka Pit. Deep-Sea Research Part I - Oceanographic Research Papers 51 (11), 1457–1474.

Vilibic, I., Orlic, M., 2002. Adriatic water masses, their rates of formation and transport through the Otranto Strait. Deep Sea Research Part I - Oceanographic research papers 49 (8), 1321–1340.

Vilibic, I., Supic, N., 2005. Dense water generation on a shelf: the case of the Adriatic Sea. Ocean Dynamics 55 (5-6), 403–415, 12th International Biennial Conference on Physics of Estuaries and Coastal Seas, Merida, Mexico, Oct 19-22, 2004.

Walsh, J., MAR 7 1991. Importance of continental margins in the marine biogeochemical cycling of carbon and nitrogen. Nature 350 (6313), 53–55.

Zavatarelli, M., Baretta, J., Baretta-Bekker, J., Pinardi, N., 2000. The dynamics of the adriatic sea ecosystem. - an idealized model study. Deep Sea Research Part I: Oceanographic Research Papers 47 (5), 937–970.

Zavatarelli, M., Pinardi, N., Kourafalou, V., Maggiore, A., 2002. Diagnostic and prognostic model studies of the Adriatic Sea general circulation: Seasonal variability. Journal of Geophysical Research - Oceans 107 (C1).

Zavatarelli, M., Raicich, F., Bregant, D., Russo, A., Artegiani, A., DEC 1998. Climatological biogeochemical characteristics of the Adriatic Sea. Journal of Marine Systems 18 (1-3), 227–263.

Zehr, J. P., Ward, B. B., 2002. Nitrogen cycling in the ocean: New perspectives on processes and paradigms. Applied and Environmental Microbiology 68 (3), 1015–1024.

Zore-Armanda, M., Gacic, M., FEB 1987. Effects of Bura on the circulation in the North Adriatic. Annales Geophysicae Series B - Terrestrial and Planetary Physics 5 (1), 93–102.

Zweifel, U. L., Norrman, B., Hagstrom, A., 1993. Consumption of dissolved organic carbon by marine bacteria and demand for inorganic nutrients. Marine ecology. Progress series (1-2), 23–32.

THE PRESENT RESEARCH WORK HAS BEEN (PREPARED TO BE) PUBLISHED IN:

..... (FULL REREFENCE OF THE ARTICLE/COMMUNCATION/ TECHNICAL REPORT)
.....
.....
.....
.....
.....
.

Joint European MSc Degree

European MSc in Marine Environment and Resources

QUALITY AWARD
MICINN 2008-2012 **Ref MO2006-00744**

Dr ....Jon Saenz.....
as teaching staff of the MER Master of the University of .....Pais Vasco.....

CERTIFIES:

That the research work entitled. ....
"A mechanistic study of the low trophic level ecosystem structure in the coastal zone".....
has been carried out by .....Giulia Mussap.....
in:
SiNCEM Laboratory
Corso di Scienze Ambientali
University of Bologna
Via S.Alberto 163
48100 Ravenna, Italy
Tel: +39-0544-937322
Fax: +39-0544-937323
under the supervision of Prof Nadia Pinardi...
from the of the...University of Bologna...

in order to achieve 30 ECTS as a part of the MER Master program.

In ....., September 2012

Signed: Presenter (.....).

Supervisor Nadia Pinardi .....